AD-A072 157 COLD REGIONS RESEARCH AND ENGINEERING LAB HANOVER NH F/G 13/2
DETECTION OF ARCTIC WATER SUPPLIES WITH GEOPHYSICAL TECHNIQUES,(U)
JUN 79 S A ARCONE, A J DELANEY, P V SELLMANN

UNCLASSIFIED CRREL-79-15 NL

| OF |
AD
A072157

END
DATE
FILMED
9-79
DDC

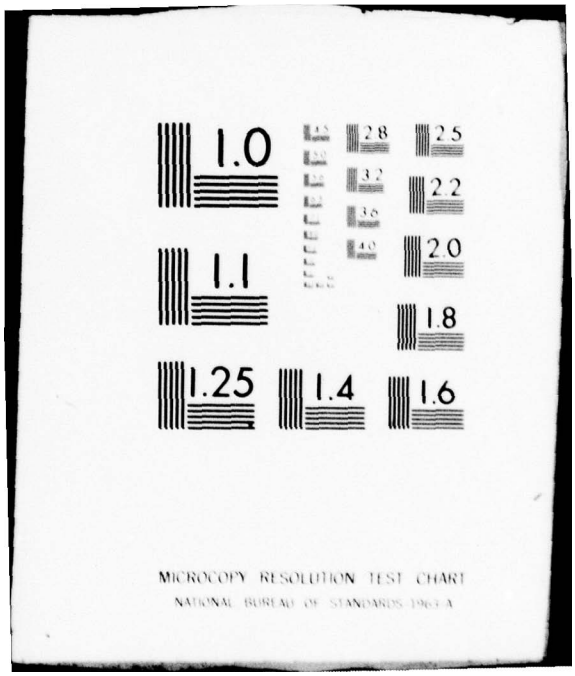
1.0
1.1
1.25
1.4
1.6
2.8
3.2
3.6
4.0
2.5
2.2
2.0
1.8
MICROCOPY RESOLUTION TEST CHART
NATIONAL BUREAU OF STANDARDS 1963-A

CRREL

REPORT 79-15

LEVEL II

Detection of arctic water supplies with geophysical techniques

For conversion of SI metric units to U.S./British customary units of measurement consult ASTM Standard E380, Metric Practice Guide, *published by the American Society for Testing and Materials, 1916 Race St., Philadelphia, Pa. 19103.*

Cover: Use of the EM-31 magnetic induction (left) and EM-32 surface impedance resistivity instruments (described in text).

(14)

CRREL [redacted]-79-15

(6)

Detection of arctic water supplies with geophysical techniques

(10)

S.A./Arcone, A.J./Delaney [redacted] P.V./Sellmann

(11) Jun[redacted]979

(12) 36p.

(16) 4A762730AT42

(17) A3

Prepared for
DIRECTORATE OF MILITARY PROGRAMS
OFFICE, CHIEF OF ENGINEERS
By
UNITED STATES ARMY
CORPS OF ENGINEERS
COLD REGIONS RESEARCH AND ENGINEERING LABORATORY
HANOVER, NEW HAMPSHIRE, U.S.A.

037100

Unclassified

SECURITY CLASSIFICATION OF THIS PAGE (When Data Entered)

REPORT DOCUMENTATION PAGE

READ INSTRUCTIONS BEFORE COMPLETING FORM

1. REPORT NUMBER: CRREL Report 79-15

2. GOVT ACCESSION NO.

3. RECIPIENT'S CATALOG NUMBER

4. TITLE (and Subtitle): DETECTION OF ARCTIC WATER SUPPLIES WITH GEOPHYSICAL TECHNIQUES

5. TYPE OF REPORT & PERIOD COVERED

6. PERFORMING ORG. REPORT NUMBER

7. AUTHOR(s): S.A. Arcone, A.J. Delaney and P.V. Sellmann

8. CONTRACT OR GRANT NUMBER(s)

9. PERFORMING ORGANIZATION NAME AND ADDRESS: U.S. Army Cold Regions Research and Engineering Laboratory, Hanover, New Hampshire 03755

10. PROGRAM ELEMENT, PROJECT, TASK AREA & WORK UNIT NUMBERS: DA Project 4A762730AT42, Technical Area A3, Work Unit 009

11. CONTROLLING OFFICE NAME AND ADDRESS: Directorate of Military Programs, Office, Chief of Engineers, Washington, D.C. 20314

12. REPORT DATE: June 1979

13. NUMBER OF PAGES: 34

14. MONITORING AGENCY NAME & ADDRESS (if different from Controlling Office)

15. SECURITY CLASS. (of this report): Unclassified

15a. DECLASSIFICATION/DOWNGRADING SCHEDULE

16. DISTRIBUTION STATEMENT (of this Report)

Approved for public release; distribution unlimited.

17. DISTRIBUTION STATEMENT (of the abstract entered in Block 20, if different from Report)

18. SUPPLEMENTARY NOTES

19. KEY WORDS (Continue on reverse side if necessary and identify by block number)

Arctic regions
Electrical resistivity
Geophysics
Water supplies

20. ABSTRACT (Continue on reverse side if necessary and identify by block number)

This report discusses the application of several modern geophysical techniques to groundwater exploration in areas of permafrost. These methods utilize the principles of magnetic induction and radiowave surface impedance in the 10- to 400-kHz band, the techniques of impulse and side-looking radar in the 50- to 10,000-MHz band, and also some optical techniques using imagery obtained from a satellite. Low frequency case studies demonstrate the use of the techniques for detecting free water under an ice cover in shallow, almost completely frozen lake basins, and thaw zones within lake beds, stream channels, and in permafrost in general. The radar studies demonstrate the use of these techniques for determining depth of free water and ice cover thickness on lakes and rivers.

DD FORM 1 JAN 73 1473 EDITION OF 1 NOV 65 IS OBSOLETE

Unclassified

SECURITY CLASSIFICATION OF THIS PAGE (When Data Entered)

PREFACE

This report was prepared by Dr. Steven A. Arcone, Geophysicist, and Allan J. Delaney, Physical Sciences Technician, of the Physical Sciences Branch, Research Division, and by Paul V. Sellmann, Geologist, of the Geotechnical Research Branch, Experimental Engineering Division, U.S. Army Cold Regions Research and Engineering Laboratory.

The funding for the research described in this report was provided by DA Project 4A762730AT42, *Design, Construction and Operations Technology for Cold Regions*, Technical Area A3, *Facilities Technology*, Work Unit 009, *Water Supply for Cold Regions*.

Dr. Daniel Lawson and Dr. William St. Lawrence of CRREL technically reviewed the manuscript of this report.

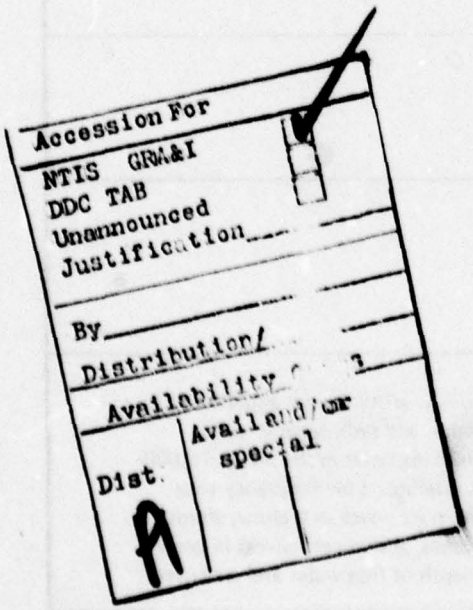

CONTENTS

ILLUSTRATIONS

DETECTION OF ARCTIC WATER SUPPLIES WITH GEOPHYSICAL TECHNIQUES

S.A. Arcone, A.J. Delaney and P.V. Sellmann

INTRODUCTION

Groundwater distribution patterns in arctic regions are similar to, but more restricted than, those in geologically analogous permafrost-free areas (Hopkins et al. 1955). Where permafrost exists, the distribution of groundwater can be directly related to thaw zone occurrence, which depends on the physiographic setting (slope, exposure, vegetation, soil type, proximity to major water bodies, etc.), mean annual air temperature, and historical factors. However, establishing the distribution of thaw zones alone does not assure a developable source of water. The sediments should ideally be coarse-grained and extensive, and the water itself should be free of organic and mineral pollution.

Situations that exhibit a potential for water development in permafrost areas are: 1) unfrozen permeable materials above, within and/or below the permafrost, 2) ponds, lakes and rivers that do not freeze to the bottom in the winter and are deep enough to provide a supply of water without high concentrations of impurities, and 3) unfrozen zones below river and lake bottoms where a reservoir of water may be available in permeable material. Most of these situations represent an interruption in permafrost distribution or can be related to ice thickness of water bodies, suggesting that their occurrence should decrease as one moves progressively north.

There are many geophysical exploration methods available to aid in locating thaw zones in permafrost, and therefore these techniques could be applicable to groundwater surveys. These methods identify material types by determining physical properties such as acoustic velocities (the seismic method) or electrical resistivity (galvanic electromagnetic methods). Examples of groundwater investigations in nonpermafrost areas using these methods include the location of buried stream channels, determinination of the position of the water table, and studies of coastal salt water intrusion. Recent surveys of the extensive literature and techniques utilized for groundwater detection in both permafrost and nonpermafrost areas have been made by Zohdy et al. (1974) and Ogilvy (1967).

Electromagnetic methods* of geophysical exploration have become popular since the early to mid 1960's because of their noncontact nature (i.e. lack of earth-electrode contact and its inherent resistivity problems) and their well-defined depths of penetration. These methods utilize propagating electromagnetic energy from the entire known frequency spectrum: from ultra low frequency signals generated by lightning to gamma-ray radiation produced by radioactive decay. Methods may be either passive, such as in the detection and measurement of telluric currents, self-potentials, magnetic fields and optical and nuclear radiation, or they may be active, such as in the transmitting and receiving of radar signals or radiowaves and in the induction and measurement of magnetic fields and electric field polarization. In all electromagnetic

*Also called a.c. or alternating current methods.

geophysical methods, the physical property measured usually depends on the frequency used. General information on most methods is given in Barnes (1965), Ogilvy (1967), Zohdy (1974), and Ward (1967).

The propagation of electromagnetic energy up to about 3×10^{10} Hz in earth materials depends strongly on electrical resistivity (the inverse of conductivity) and on dielectric properties. Propagation also depends on geometric considerations, such as comparison of wavelength to the size of the feature being investigated. Resistivity and dielectric properties are strongly influenced by the presence of water, because the dissolved ions can make a conductive, polarizable electrolyte. Below about 1 MHz, resistivity is the predominant property. Resistivity surveys can provide information on the distribution and quality of subsurface water, providing that resistivity contrasts exist between the water or water-bearing strata and the other surrounding materials. Above about 100 MHz, dielectric properties are most important. Although present systems (interferometric and radar) are rarely used for measuring dielectric properties, their performance depends on interfacial dielectric contrasts, thus enabling continuous profiling.

In this report we review the theory and application to arctic groundwater problems of several active techniques used in the radiowave band between 15 kHz and 10 GHz. The studies presented are extracted from research projects that we and our colleagues at CRREL and the Geological Survey of Canada have performed over the past several years. The discussions of data interpretation are limited to brief descriptions of material type correlations with resistivity readings or with signal strengths. More thorough discussions of electromagnetic field penetration, interpretation of stratification, and the effects of topography, lateral inhomogeneity and material type may be found in the references cited with each example.

The body of this report is divided into two parts. Part I deals with low frequency (15 to 400-kHz) radiowave and magnetic induction resistivity methods. Part II deals with high frequency (0.1- to 10-GHz) radar dielectric methods. Each part begins with a discussion of the appropriate earth electrical properties, followed by a description of the principles and equipment used and documented studies appropriate to arctic groundwater investigation.

A review of a CRREL study of NASA satellite imagery over arctic lakes is presented in Appendix A. Although photographic imagery does not directly reveal subsurface information, it is included because of its application to arctic groundwater problems.

PART I. LOW FREQUENCY RESISTIVITY METHODS

Resistivity of earth materials

The geophysical systems to be discussed in this section measure the physical property of electrical resistivity at frequencies below about 1 MHz. We therefore begin with a discussion of the electrical resistivity of earth materials with emphasis on materials in a frozen state. The property of dielectric permittivity has a negligible effect on propagation at the frequencies considered, while the property of magnetic permeability is essentially the same in most materials throughout nature, the major exceptions being a few iron-bearing minerals. More complete discussions of electrical properties of earth materials may be found in the texts by Keller and Frischknecht (1966) and Parkhomenko (1967).

The electrical resistivity (or its inverse, conductivity) of a material is a bulk property expressed in ohm-meters. It is generally inversely proportional to the product of the concentration of charge carriers and their mobility. Charge carriers are termed either electronic when they are electrons (as in a metal), or electrolytic when they are ions (such as dissolved salts). The mobility of the charge carriers is determined by many factors, such as temperature, the viscosity of the dissolving fluid, the weight of the ion, or the texture of the material through which the ionic solution must pass.

Generally natural material resistivity is determined by texture (grain size, porosity and permeability) and the ionic concentration within the adsorbed water on grain surfaces and within the absorbed water in pore spaces. Electrical conduction in rocks and sediments is therefore mainly electrolytic and takes place along continuous films of water adsorbed on grain boundaries, as well as through water that may fill the available pore spaces. A major mineralogical consideration is that clays can have a large

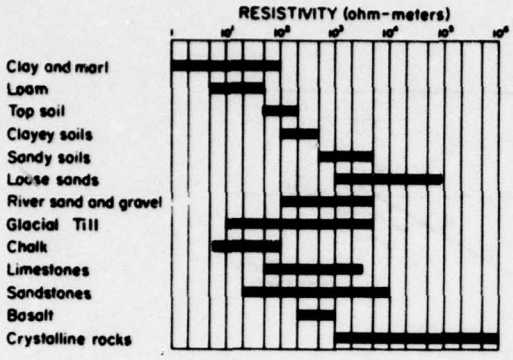

Figure 1. Resistivity ranges of most unfrozen earth materials (after Culley et al. 1975).

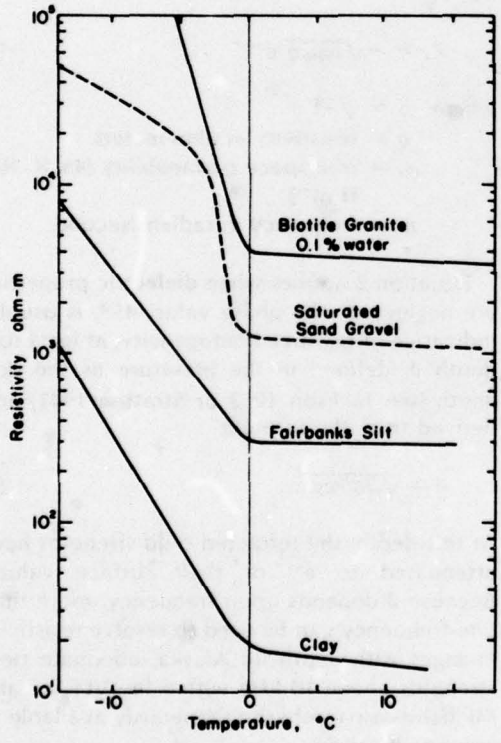

Figure 2. Resistivities of several saturated soil types and one rock type as a function of temperature (compiled by Hoekstra et al. 1974).

amount of ions adsorbed on their crystal lattices, producing a surface conduction effect that can appreciably lower the resistivity of a sediment or rock.

In Figure 1 the expected ranges of resistivity based on surveys and laboratory measurements are compiled for some unfrozen earth materials. Among the unconsolidated materials, clay and marl through loose sands generally show an increase in resistivity with increase in particle size. This may be expected because of the corresponding decrease in available adsorbing surface area. Alluvial deposits and glacial till exhibit a wide range of resistivities due to large variations in textural composition. The consolidated materials, chalk through crystalline rocks, generally show an increase in resistivity with decreasing porosity and permeability. Clay content may also be significant in some rock types (Ward 1967), and the large amounts of iron- and magnesium-rich minerals in some basaltic igneous rocks can make them less resistive than granitic igneous types. In all cases, the effects of weathering, jointing or fracture, which increase permeability and cause the formation of clay minerals, significantly lower the resistivity of the fresh rock.

In frozen soils, temperature and ice content greatly influence electrical resistivity. At temperatures above freezing, only small increases in resistivity may take place with decreasing temperature. Below freezing, however, temperature changes can cause substantial increases in resistivity, as is illustrated in Figure 2 for several saturated sediment types and one rock type. Below 0°C, the increase in resistivity is due to the decrease in the amount of unfrozen water remaining in the ground (Hoekstra and McNeill 1973, Anderson and Morgenstern 1973). As this unfrozen water is in the adsorbed state, resistivity generally decreases with decreasing grain size (or increasing area of surface adsorption) as it does for unfrozen sediments.

Frozen ground may also have ice contents in excess of saturation, as is shown by the occurrence of massive ice lenses and ice wedges which commonly occur in fine-grained sediments. Hoekstra et al. (1974) investigated the relationship of resistivity to ice volume for Fairbanks silt and found an approximate linear dependency, with electrical resistivity varying from about 2500 ohm-m to greater than 100,000 ohm-m for ice volumes between 60 and 100%.

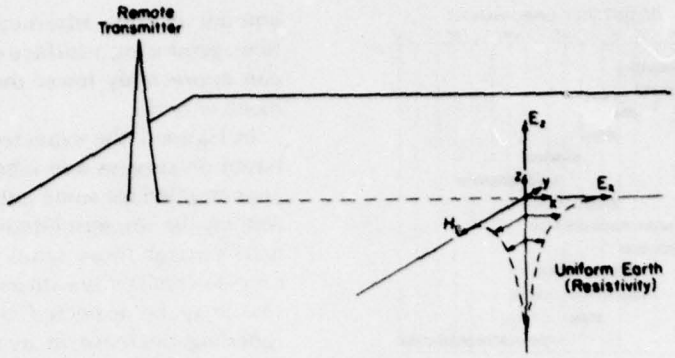

Figure 3. Ground electromagnetic field components of a radio wave transmitted from a vertically polarized antenna.

Theory and description of techniques

Surface impedance (radiowave) technique

The surface impedance technique derives ground resistivity values from a comparison between the electromagnetic field components of a propagating ground or sky wave. Between 15 and 25 kHz in the VLF (very low frequency) band, powerful transmitters operated for military communications allow radiation to be monitored over a range of several thousand kilometers via the sky modes, which consist of waves singly or multiply reflected from the ionosphere and the earth. Station NLK (18.6 kHz) in Jim Creek, Washington, is usually monitored throughout Alaska. Between 200 and 415 kHz, numerous low power transmitters operated for small plane navigation allow radiation to be monitored only within their immediate vicinity. This radiation is in the ground wave mode wherein the radiation spreads radially over the ground from the transmitter whose range is dependent on ground resistivity.

The electromagnetic field components of a ground or sky wave radiated by a vertically polarized antenna are illustrated in Figure 3. *E* refers to the electric field components and *H* to the magnetic field component referenced to local x, y, z coordinates. The surface impedance Z_s is then defined as*

$$Z_s \triangleq E_x/H_y|_{z=0}. \quad (1)$$

*This definition automatically applies to the ground wave, but for the sky wave the grazing incidence angle upon the earth must be near 0°, which is usually true at ranges > 1000 km at VLF.

Z_s is a complex quantity having both an amplitude $|Z_s|$ and a phase ϕ expressible as $Z_s = |Z_s| e^{i\phi}$. At frequencies below about 1 MHz, Z_s is approximated for a uniform subsurface model by

$$Z_s = -\sqrt{\omega\mu_0\varrho}\, e^{i45°} \quad (2)$$

where $i = \sqrt{-1}$
ϱ = resistivity in ohm-meters
μ_0 = free space permeability ($4\pi \times 10^{-7}$ H m^{-1})
ω = frequency in radians/second.

Equation 2 applies when dielectric properties are neglected. The phase value, 45°, is usually indicative of resistive homogeneity, at least to a depth δ, defined in the literature as the skin depth (see Jackson 1962 or Stratton 1941) and derived from the formula

$$\delta = \sqrt{2\varrho/\omega\mu_0}. \quad (3)$$

At this depth, the refracted field strengths have attenuated to e^{-1} of their surface values. Because δ depends upon frequency, more than one frequency can be used to resolve resistivity changes with depth. In Alaska, adequate field strengths above 10 kHz within the VLF, LF and MF bands are rarely simultaneously available at any one location.

When the earth is layered, eq 2 must be modified because the phase and amplitude of Z_s change, with the magnitude of change depending upon the resistivity and thickness of each layer. Wait (1962) presents formulas for generating Z_s values above any number of

layers. In general, a phase greater than 45° usually indicates that resistivity is decreasing with depth, whereas a phase less than 45° usually indicates that resistivity is increasing with depth. According to this simplified model of homogeneous layers, all phase angles occur between 0° and 90°. When lateral inhomogeneities exist, the theory does not apply and only qualitative interpretations can be made.

The instruments used for measuring resistivity in the VLF and LF bands are similar to each other and commercially available. E_x is determined between two probes inserted in the ground and compared to H_y measured with a ferrite-loaded coil. The LF device must be pretuned for operation between 200 and 400 kHz, whereas the VLF device operates with pretuned circuits, each pretuned to one of the few VLF transmitters in use today. The amplitude of Z_s is calibrated in ohm-meters of apparent resistivity ϱ_a (range is 0-30,000 ohm-m) which is determined from the amplitude inversion of eq 2:

$$\varrho_a = |Z_s|^2/\omega\mu_0. \qquad (4)$$

This value equals the true resistivity when the earth is homogeneous. The phase of Z_s is read directly in degrees (range is 0° to 90°). A high impedance voltmeter is used to measure E_x so that the contact resistance of the probes does not interfere with the measurement.

The accuracy of the readings depends upon the signal-to-noise ratio. This ratio is mainly determined by transmitter distance and power (for LF and VLF), by ionospheric factors (for VLF), and by the value of ground resistivity itself (for LF and VLF) because as resistivity decreases so does the amplitude of E_x.

Airborne radiowave technique

The surface impedance resistivity method has also been adapted to airborne use (Hoekstra and McNeill 1973, Hoekstra et al. 1974). In this method, however, E_x is compared to E_x rather than H_y (see Fig. 3) because E_x cross-couples during aircraft roll into the horizontal antenna that measures E_x. Consequently, only the component of E_x that is out of phase with E_x can be used. E_x is then used as the phase and amplitude reference against which E_x is measured so as to avoid making measurements of the absolute electric field strength, which varies with range, ionospheric factors, etc. (this is discussed more thoroughly in Arcone 1977). The disadvantages, then, of this system are that only a partial measure of the apparent resistivity is obtained with no phase information, and that there is a loss of ground detail due to altitude effects. The advantage is the greater amount of area that can be covered.

Magnetic induction technique

This method derives ground resistivity values from the amount of magnetic field coupling between two loop antennas located at or slightly above the earth's surface. One loop, the transmitter, generates a primary a.c. magnetic field that couples directly to the receiver loop through free space and also induces eddy currents within the earth. These currents then generate a secondary magnetic field that also couples with the receiver and is used in comparison with the primary field for computing resistivity values. This secondary field is not in phase with the primary field, and thus it has both in-phase and quadrature phase components with respect to the primary field. The quadrature phase component is used for computing resistivity values because it has a greater range of linear response with resistivity. In addition to ground resistivity, secondary coupling is also affected by loop separation and orientation, loop height above ground, and transmitter frequency.

The Geonics EM-31 was used for the magnetic induction surveys. This instrument is calibrated in millisiemens/meter of apparent conductivity σ_a ($\sigma_a = 1/\varrho_a$). At the instrument's operating frequency of 40 kHz, the apparent conductivity with respect to a first layer thickness t for a two-layer model varies as is shown in Figure 4. σ_a is normalized by the conductivity of the first layer and t is normalized by the coil separation s = 3.66 m. As shown in Figure 4, when a conductor lies above an insulator ($\sigma_2/\sigma_1<1$), little change in σ_a will occur for values of $t/s>2$ (or t = 7.3 m for the EM-31).

Case studies

Geophysical field investigations conducted by CRREL since 1971 have been performed primarily in permafrost environments. Some investigations have been conducted in temperate areas at the request of other agencies. Many aspects of these studies are applicable to arctic groundwater investigations and are therefore presented. The studies provide information on

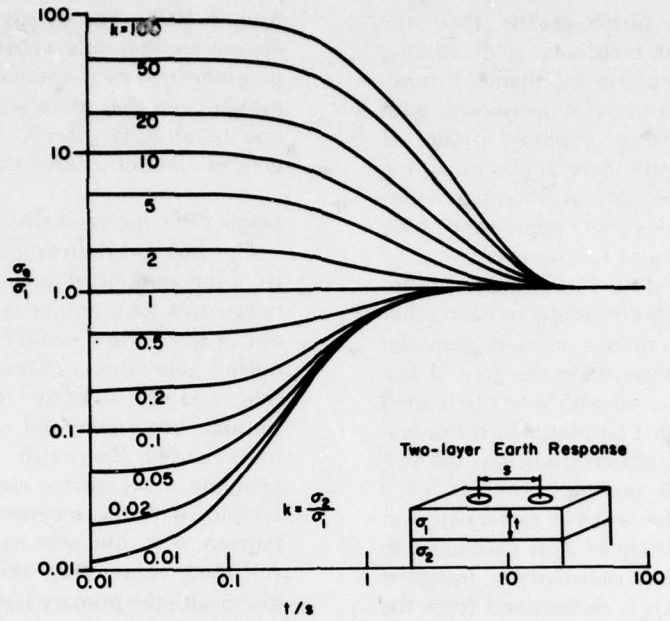

Figure 4. Two-layer curves for a coplanar, double loop magnetic induction system operating at a frequency of 40 kHz. For the Geonics EM-31, s = 3.66 m. (Courtesy of Geonics Ltd.)

water below lake and river ice, thaw zones below the beds of streams and lakes, unfrozen zones in permafrost areas, and distribution of materials that have high permeability and may provide good groundwater sources.

Location of thaw zones beneath lakes and rivers

Smith Lake, Fairbanks, Alaska. Smith Lake is about 10 km west of Fairbanks in the discontinuous permafrost zone. The permafrost, a frozen silt, surrounds the lake (Péwé 1958). At the time of the surveys, lake ice thickness varied between 66 and 76 cm and water depth increased gradually from the margins to the center where the depth was approximately 2 m including the ice.

The lake was investigated in April 1974 using the surface impedance method at 18.6 kHz and in April 1977 using the magnetic induction (EM-31) method. Over the central portion of the lake, two VLF readings gave 110 and 120 ohm-m at 45° (very few readings were successful due to the weak reception in the area) while the magnetic induction readings made at 3-m intervals (Fig. 5) ranged between 130 and 180 ohm-m. Over the permafrost, one VLF measurement was read at between 500 and 1000 ohm-m at about 45°, while the EM-31 readings ranged from 400 to 700 ohm-m.

The VLF data imply deep thaw under the lake and probably no permafrost. At 120 ohm-m, the skin depth at 18.6 kHz is 40 m which is close to the maximum permafrost thickness in other parts of this area. The magnetic induction resistivities are greater here because of the greater sensitivity to the ice cover and because the instrument was held at a 1-m height. This is verified in Figure 6 which shows that a model 120-ohm-m real resistivity for the water and thawed bottom sediments rises to a 165-ohm-m apparent resistivity with an ice cover, which is typically about 6000 ohm-m. Increases in ice resistivity above about 1000 ohm-m marginally affect the readings.

Although Smith Lake has over 1 m of unfrozen water remaining near its center during late winter, the resistivity data do not indicate its presence in spite of giving information on depths of thaw. This is due to the lack of resistivity contrast between the water and sediments or even within the sediments themselves.

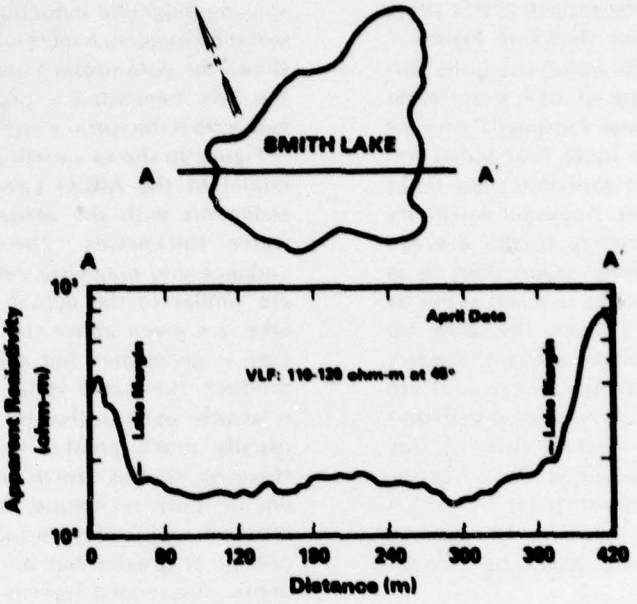

Figure 5. Magnetic induction apparent resistivity traverse over Smith Lake, near Fairbanks, Alaska.

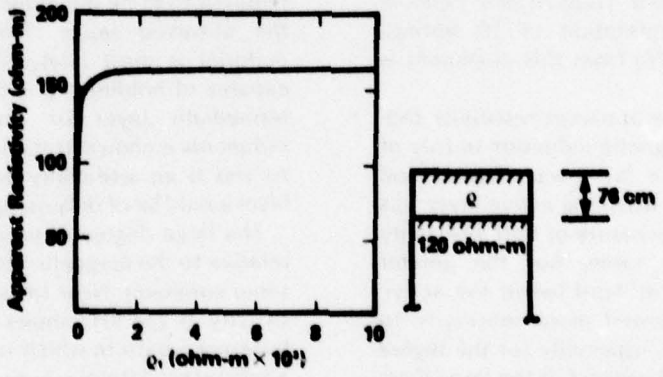

Figure 6. Magnetic induction apparent resistivity as a function of ice resistivity for a lake model in which water and bottom sediments are of the same resistivity. Resistivity variations above 1000 ohm-m in the ice cover have marginal effect upon the apparent resistivity.

Thaw lakes, near Pump Station 5, Alyeska Pipeline Route, Alaska. The results of this study (Sellmann et al. 1974) are shown in Figure 7. Resistivity profiles (Fig. 7b and c) using the surface impedance technique at VLF were made across two small lakes near Prospect Camp on the Trans-Alaska Pipeline route near pump station 5 (Fig. 7a). These are probably thaw lakes surrounded by permafrost. Apparent resistivity readings over the surrounding tundra average about 500 ohm-m, but these values drop to as low as 15 ohm-m along section a-a' and as low as 50 ohm-m along section E-B over the lakes. No investigation was made of the amount of water under the ice or of the depth of thaw beneath the bed. However, the very low resistivities measured along a-a' are characteristic of clay and silt, implying that some thaw exists. Therefore, if water is present under the ice, it probably occurs in thawed, fine-grained sediments from which water would be difficult to extract.

Lake bed, Gulkana, Alaska. This study (Arcone et al. 1978) was conducted at a small lake located near the town of Gulkana (Fig. 8). The soil types of the area are generally described as glacial clays, clay tills and lacustrine deposits that are fairly homogeneous in nature except for their ice content. The site is situated along one of the earlier proposed Trans-Alaska Pipeline alignments. An interpretation of 25 borings (R&M Engineering 1970) from this alignment is presented in Figure 8b.

Figure 8a shows the apparent resistivity profiles measured by magnetic induction in July of 1976 when the active layer was thawed and again in April of 1977 when the active layer was frozen. The qualitative nature of both resistivity profiles remains the same, but the greater penetration afforded in April (when the active layer was frozen) allowed more sensitivity to deeper soil variations, especially for the higher ice content regions. The effect of the large thaw zone at the center is to lower the apparent resistivity to less than 50 ohm-m during both observation periods. This low value of resistivity is indicative of the fine-grained sediments of the thaw zone and probably indicates a poor water supply. It is similar to the thaw zone discussed previously.

Thaw lake, Alaskan Arctic Coastal Plain. A comparative survey was conducted at an artificially deepened lake near Prudhoe Bay, Alaska, situated next to the Sagavanirktok River. Resistivity was measured using the 3.7-m coil spacing magnetic induction instrument and the surface impedance method at 234 kHz. Figure 9a shows the data profiles and the cross section of the lake beneath the profiles. Also shown in Figure 9a is the surface impedance phase profile.

Figure 9b shows a vertically layered resistivity model of the ARCO Lake and its subsurface sediments with the actual values of ice and water thicknesses. Theoretical surface impedance and magnetic induction values, which are similar to the actual data taken over the lake, are given above the model. A three-layer case is given here but other models may also produce the same data. The upper layer is relatively pure freshwater ice with resistivities usually much greater than the value given. However, for this case of an insulator over a conductor, both techniques are insensitive to the resistivity value of the insulator when it is 10,000 ohm-m or greater but are sensitive to the ice depth. The second layer is of fresh water but at an unusually low resistivity value of 40 ohm-m, suggesting that the water has a very high ion content. The third layer is thawed sediment which may be as deep as 20 to 30 m. This material is composed primarily of sands and gravels for which 1000 ohm-m is not unreasonable. In this case, the value of 1000 ohm-m was required to bring the model phase data well into the observed range. Therefore, this thawed material is most likely highly permeable and capable of holding a great deal of water. No intermediate layer of fine-grained lacustrine sediments is shown at the lake bed in the model. As this is an artificially deepened lake, such a layer would be of only marginal thickness.

The large degree of variability in the LF data relative to the magnetic induction data deserves some comment. Near the shore the apparent resistivity at 234 kHz shows a very interesting interference pattern which is usually indicative of a subsurface lateral inhomogeneity in resistivity. Over the central portion of the lake, however, the source of the variability is not certain. One possibility is an uneven distribution in thickness and/or resistivity of the bottom sediments. Note that the lowest values of resistivity are associated with the highest values of phase, which is theoretically correct in view of the resistivity stratification (see, for example, Arcone et al. 1978).

Thawed river channels - Sagavanirktok and Kuparuk Rivers. Small water bodies can usually

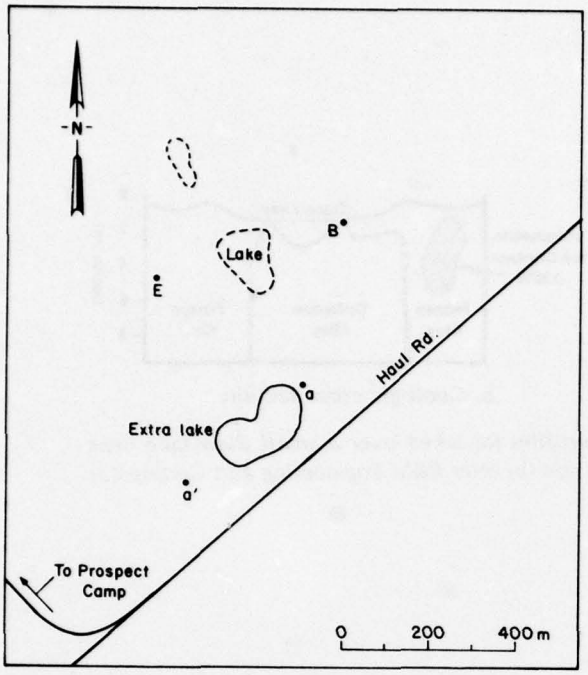

a. Location map showing survey lines near pump station 5.

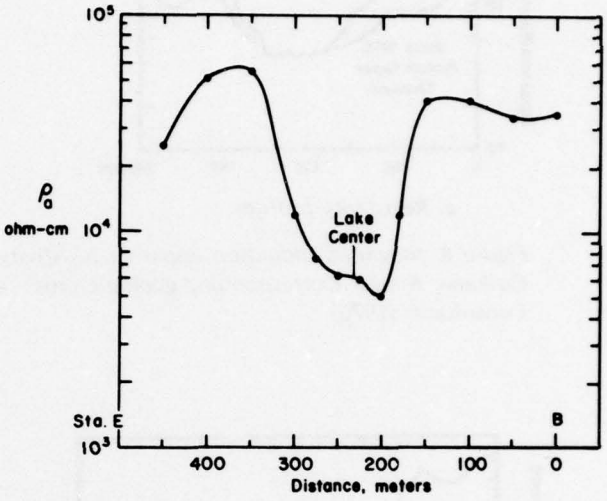

b. Apparent resistivity profile at VLF along line E-B.

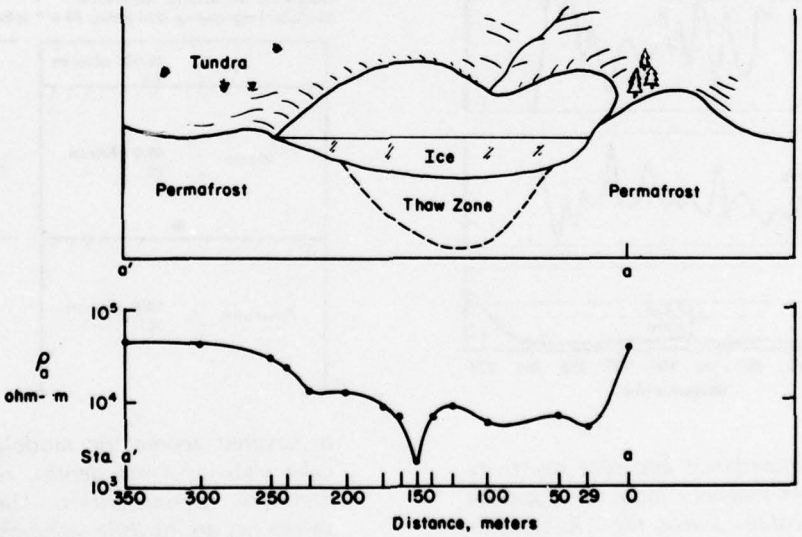

c. Idealized section and associated apparent resistivities across "Extra Lake" along line a-a'.

Figure 7. Resistivity profiles using the surface impedance technique of two thaw lakes near pump station 5, Alyeska Pipeline route, Alaska.

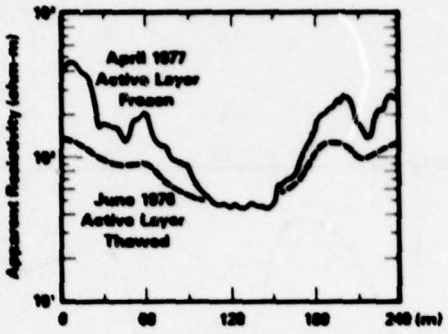

a. Resistivity profiles.

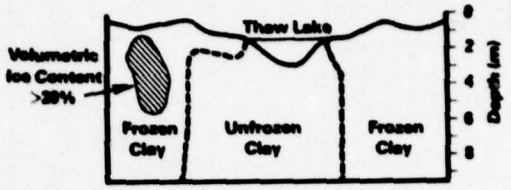

b. Geologic cross section.

Figure 8. Magnetic induction apparent resistivity profiles (a) taken over a small thaw lake near Gulkana, Alaska. Corresponding geologic cross section (b) after R&M Engineering and Geological Consultants (1970).

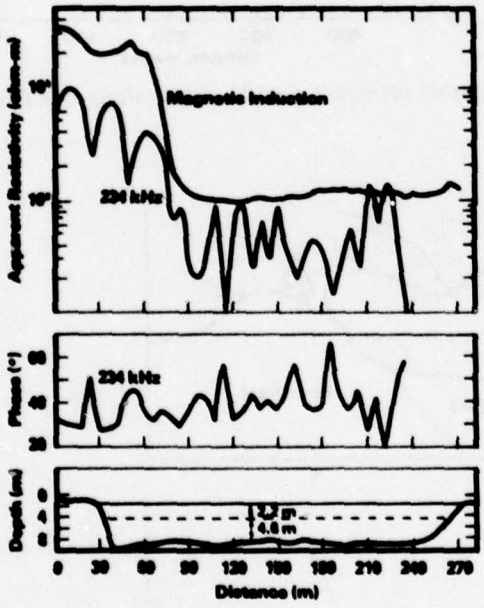

a. Surface impedance apparent resistivity and phase and magnetic induction apparent resistivity profiles across the ARCO Lake. (Approximate lake cross section along traverse from data courtesy of Austin Kovacs, CRREL).

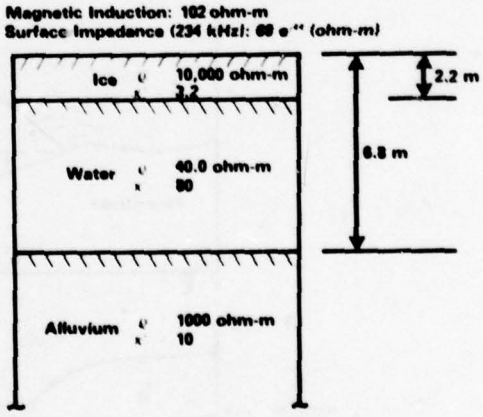

b. Layered geoelectric model of the ARCO Lake showing layer depths, resistivities and dielectric permittivities. The permittivity values (κ') are of little significance at the frequences used. The values given above the model are theoretical and are to be compared with the actual data of 9a.

Figure 9. Apparent resistivity profiles and layered geoelectric model of ARCO Lake at Prudhoe Bay, Alaska.

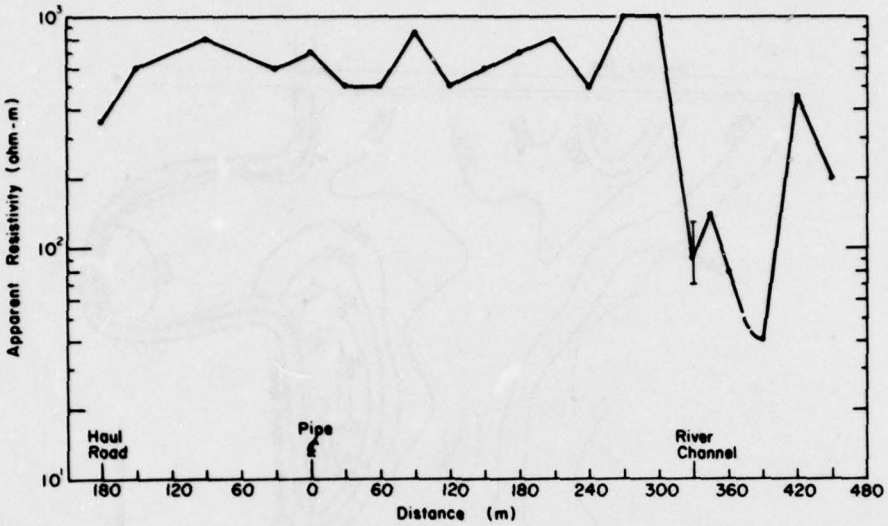

Figure 10. VLF apparent resistivity profile across the main channel of the Sagavanirktok River near Franklin Bluffs, Alaska.

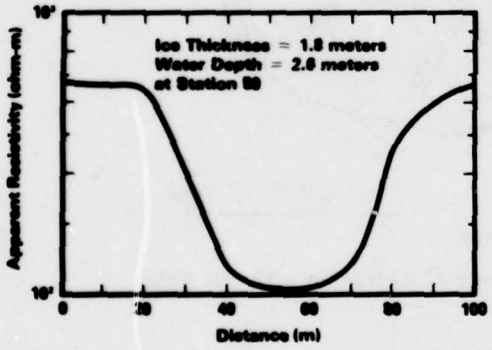

Figure 11. Magnetic induction profile across the Kuparuk River (British Petroleum Co. water supply), near Prudhoe Bay, Alaska (after Northern Engineering Services Company 1977).

be found in the winter only beneath major arctic streams because most streams freeze to their bed. Thus, seasonal discharge of arctic rivers and streams usually makes for an unreliable winter water supply. In some locations, however, the alluvium beneath the bed can be thawed to some depth, forming small reservoirs and groundwater aquifers. Geophysical techniques may then be used to detect such thaw zones since they are more conductive than the surrounding material.

Figure 10 (after Delaney et al. 1975) shows a VLF (18.6-kHz) apparent resistivity profile performed in April 1974 across the Sagavanirktok River near Franklin Bluffs in northern Alaska. The deeper and more active channel positions correspond to the lower resistivity values. The lowest values, for the channel on the left, may suggest deeper thaw.

A similar study (Fig. 11) using the magnetic induction technique was conducted by Northern Engineering Services Company (1977) and supported by a drilling program. The Kuparuk River near Prudhoe Bay, Alaska, was profiled. Resistivity minima were recorded at stations 50 and 60. At station 50, a drill hole revealed 1.8 m of ice over 2.6 m of water. At the end stations the ice was frozen to the bed.

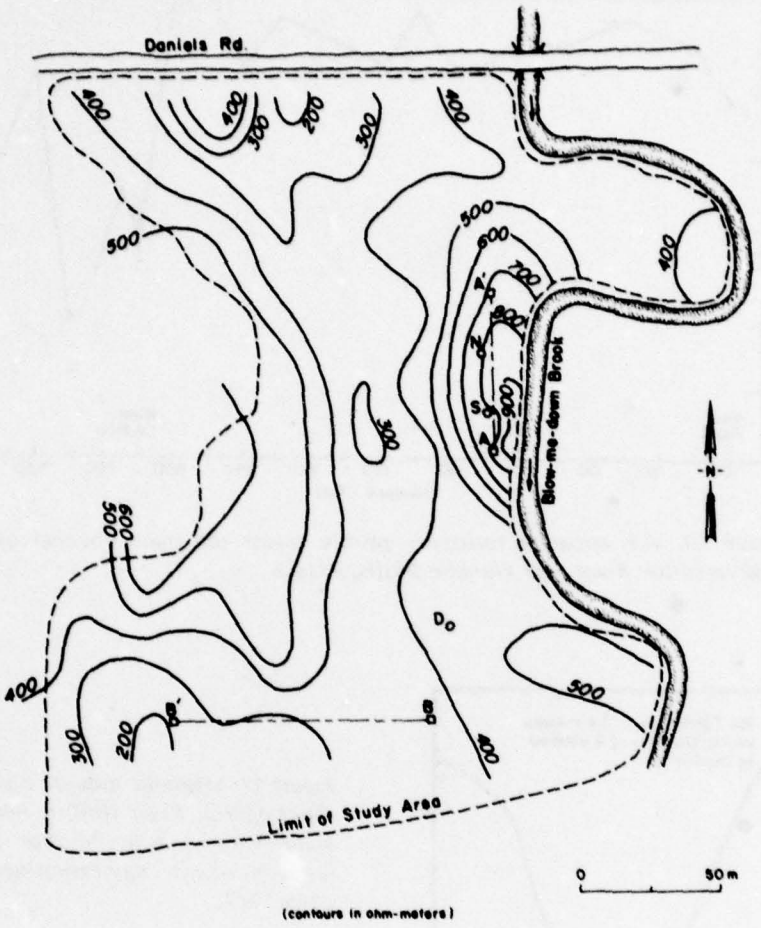

Figure 12. Apparent resistivity contours at 17.8 kHz over a 12-acre field in Plainfield, New Hampshire.

Location of permeable materials in unfrozen ground

A VLF surface impedance survey was conducted in Plainfield, New Hampshire (Delaney et al. 1974), to locate permeable material that might be recharged from a nearby stream. The area surveyed was approximately 12 acres covered by low relief glacial drift. Resistivity contours based on a 25-m grid data pattern are shown in Figure 12. Most of the area was relatively uniform in resistivity with values in the 200-400 ohm-m range. On the eastern margin of the study area adjacent to the stream, an area of higher resistivity between 500 and 900 ohm-m occurred.

Based on the range of resistivities for various earth materials shown in Figure 1, values in excess of 500 ohm-m in this type of setting can be associated with sand and gravel, materials of good permeability. Two test pits dug with a backhoe at stations N and S revealed clean gravel with a high groundwater table. A test hole drilled at station D revealed less permeable material.

Delineating permafrost boundaries

Fox, Alaska. Fairbanks and its outlying areas lie within the discontinuous permafrost zone of Alaska. This area is generally mantled with silt that overlies a Precambrian schist known as Birch Creek schist. Although the fine-grained sediments in this region do not have a potential

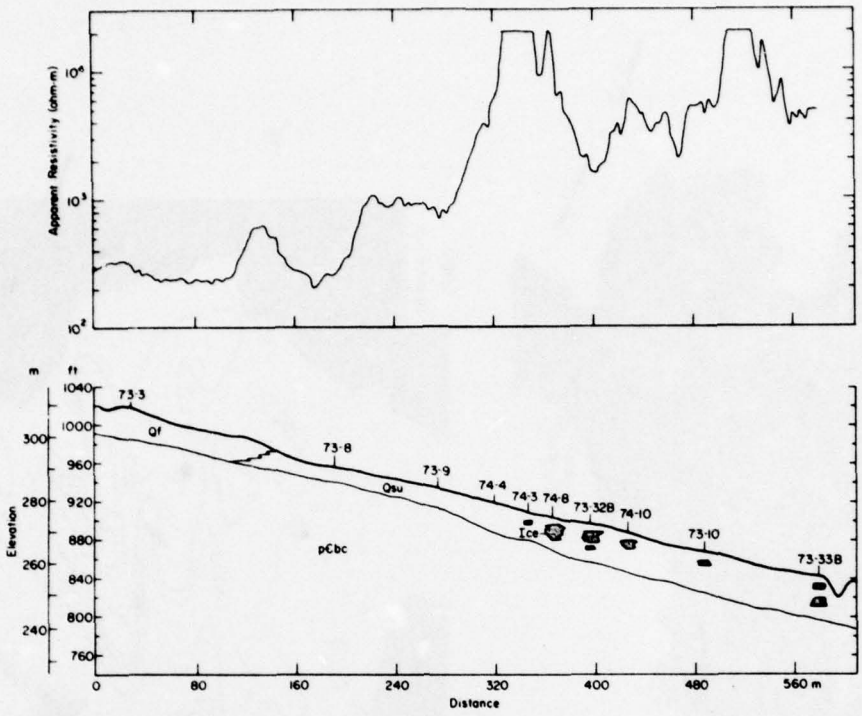

Figure 13. Apparent resistivity profile with magnetic induction along a section of the Fairbanks-Fox Road centerline, and the geological cross section derived from drill logs (numbered in the figure) provided by the Alaska Highway Department. (Qf — unfrozen silt, Qsu — frozen silt, P€bc — Birch Creek schist bedrock.)

for ground water development, the region provides many good examples of how thaw zones in perennially frozen sediments can be detected.

A 610-m linear section (Fig. 13) of the proposed Fairbanks-Fox Road near Engineer Creek was surveyed (Delaney et al. 1977) for massive ice using the magnetic induction technique. Measurements were made at 3-m intervals during early April when the surface was snow-covered and the active layer was frozen to its maximum depth. This section is on a north-facing hillside and encounters a transition from the unfrozen (Qf) to the perennially frozen (Qsu) silt units. The depth to bedrock increases fairly uniformly from 6.7 to 16.0 m and several zones of massive ice exist within the Qsu unit (borings by the Alaska Highway Department 1973, 1974). The geologic cross section was derived from the borings and the surficial geologic map of Péwé (1958).

From 0 to 120 m in the Qf unit all readings fall between 200 and 400 ohm-m, and between 120 and 280 m in the Qsu unit the readings range from 200 to 1000 ohm-m. Previous measurements made by Hoekstra et al. (1974) in the Fairbanks area using the galvanic resistivity method showed similar values for Qf and Qsu materials. Beyond 280 m in the Qsu unit, the readings increase to between 2000 and 10,000 ohm-m. This last subsection was found to contain massive ice, the distribution of which is inferred from the drill logs. The study therefore demonstrates not only the use of this technique for detecting permafrost margins but also for detecting material variations within permafrost.

Tuktoyaktuk, Canadian NWT. In April 1973, an airborne VLF survey was performed near Tuktoyaktuk, NWT, Canada, for the Geological Survey of Canada (Scott and Hunter 1976). This region is predominantly flat and underlain by

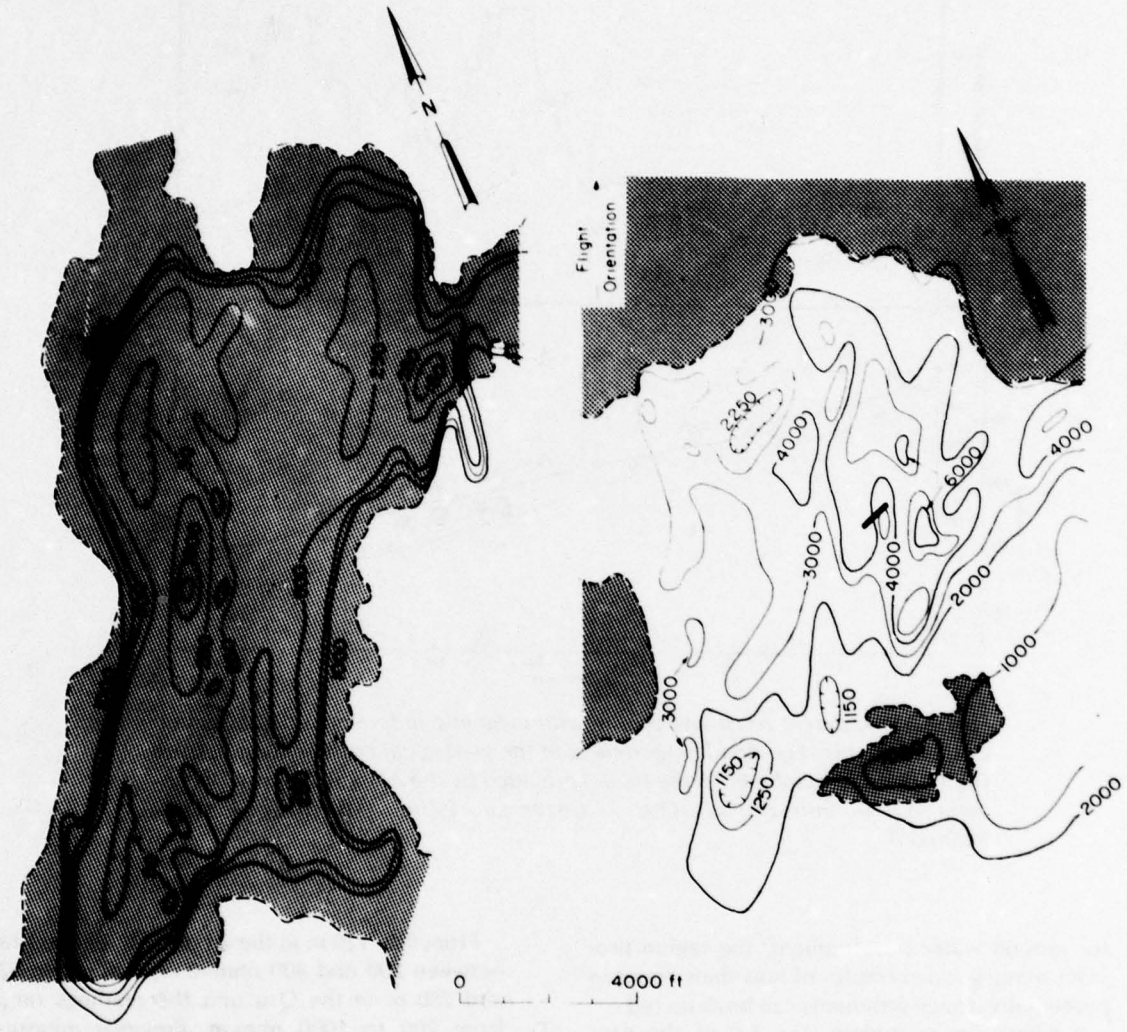

a. Thawed lake.

b. Permafrost.

Figure 14. VLF apparent resistivity contours in the Tuktoyaktuk region of the Canadian Northwest Territories above a thawed lake (a) and permafrost (b). Map courtesy of Geological Survey of Canada. Contour values are in ohm-m; shaded protions are areas of deep thaw. The heavy bar in b is where ground VLF reconnaissance was made.

ice-rich clay till. Thaw lakes occurring throughout the region have had a significant influence on development of the present landscape. Surface impedance investigations by Scott and Hunter showed areas of permafrost to have VLF apparent resistivities between 1000 and 20,000 ohm-m, but no VLF measurements were made over thaw zones.

A simplified map of contoured airborne data resistivity superimposed upon shaded areas occupied by thaw lakes is presented in Figure 14. The steep gradient in the contours of Figure 14a parallels the lake margin and thus encloses the thaw zone caused by the lake. Figure 14b shows an area just south of the area of 14a that is predominantly frozen and contains much ice near the surface. In the lower right-hand corner of Figure 14b there occurs a thaw zone with a relatively low, 1000 ohm-m contour lying directly over it. Thus, it is seen that thaw zones associated with contemporary lakes and drained lake basins may be delineated on a large scale with airborne adaptations of the surface impedance resistivity method.

PART II. HIGH FREQUENCY DIELECTRIC METHODS

Dielectric properties of earth materials

The geophysical exploration systems discussed in this section are radar systems which are used for continuously profiling or mapping surface and subsurface variations in electrical properties of earth materials. As with surface ordinance radar, the backscatter of beamed energy at frequencies usually between 100 and 10,000 MHz is monitored. Subsurface reflections take place where strong contrasts in bulk dielectric permittivity or in bulk conductivity exist. At radar frequencies, the dielectric permittivity is usually more important.

The dielectric permittivity ε is a measure of the electrical polarizability of a material and determines the velocity of propagation v in that material by the formula

$$v = 1/\sqrt{\mu\varepsilon} \tag{5}$$

where μ is the magnetic permeability of the medium which is the same as μ_0 of eq 2 for most materials. Normally, ε is expressed as

$$\varepsilon = \kappa^*\varepsilon_0 \tag{6}$$

where κ^* is the complex, relative dielectric constant that is dimensionless, and ε_0 is the dielectric permittivity of free space = 8.85×10^{-12} F/m. These units may also be expressed as (couloumb-meters/meter^2 per volts/meter) or dipole moment density per unit of electric field strength.

κ^* is a complex quantity because the polarization of a material may not always be in phase with the impressed electric field. In such situations κ^* is frequency-dependent and usually expressed as

$$\kappa^* = \kappa' - i\kappa'' \tag{7}$$

where κ' is the in-phase or real part of the dielectric constant and κ'' is the quadrature phase or imaginary part. A finite value of κ'' indicates that electromagnetic energy will be lost during propagation. The conductivity σ also causes attenuation and the two losses cannot be separated by measurement. It is then customary to define an effective quadrature phase term as σ_{eff} so that

$$\kappa^* = \kappa' - i\sigma_{eff} \tag{8}$$

where

$$\sigma_{eff} = \kappa'' + \sigma/\omega\varepsilon_0.$$

There are three ways an individual material may be polarized. First, it may have the centers of the negatively charged electron clouds of its individual atoms or molecules slightly displaced relative to the positively charged nucleus. Second, a net displacement between negative and positive ions may occur. Third, the molecules may be intrinsically polarized but oriented randomly as with water. Therefore an impressed electric field polarizes the material by giving the molecules a preferred orientation.

In composite materials, interfacial polarization may occur when the charge flow is impeded at an interface. Such phenomena are usually confined to lower frequencies than those considered in this section of the report.

It is customary to present the dispersion or frequency dependence of the complex values of κ when discussing dielectric properties. Because water is highly dispersive above 100 MHz, all water-bearing earth materials show some degree of dispersion. Figure 15 shows the dispersion of κ' and κ'' for water. The dispersion for unfrozen water results from the molecular orientation of

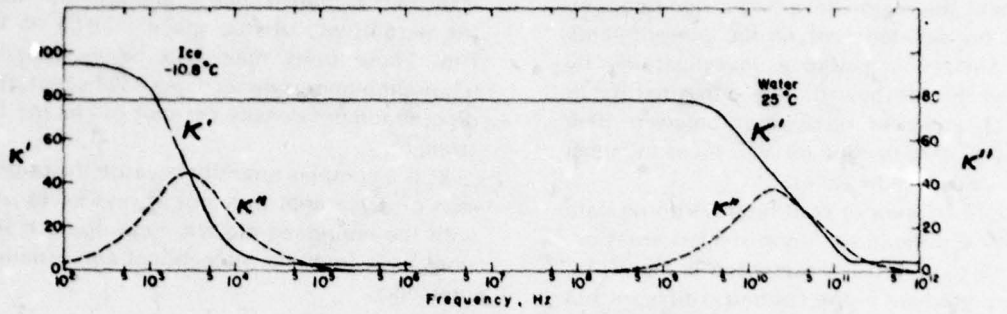

Figure 15. Relaxation spectra of water and ice (after data from Collie et al. 1948).

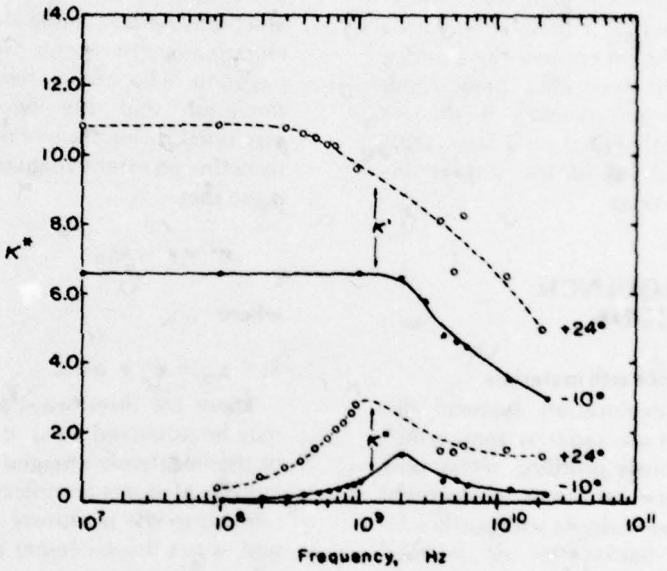

Figure 16. The complex dielectric constant of Goodrich clay at a water content of 10% (g H_2O/g soil) as a function of frequency at two temperatures (°C).

the polar water molecule, whereas the dispersion for ice results from proton migration. Both types of dispersion are described as relaxation polarizations which means that the polarization of the substance can no longer keep in phase with the applied electric field near and above some characteristic frequency.

As shown in Figure 15, the dispersion of water mainly takes place above about 200 MHz and reaches a maximum loss (i.e. maximum value of κ'') at about 20 GHz. Below about 200 MHz water is essentially lossless with a very high value of κ' at about 78. The dispersion of ice takes place at very low frequencies. Above about 0.1 MHz, ice behaves like a lossless dielectric with κ' equal to about 3.

Figures 16, 17 and 18 show the dispersions of a clay and a silty clay at different temperatures and water contents (after Hoekstra and Delaney 1974). When these curves are compared with those of Figure 15, it is evident that the range of frequencies over which the dispersion occurs is lowered from that of unfrozen water by factors between about 5 and 20, and the low frequency asymptotic values of κ' and κ'' now are between that of water and of pure sediment (κ' is about 3

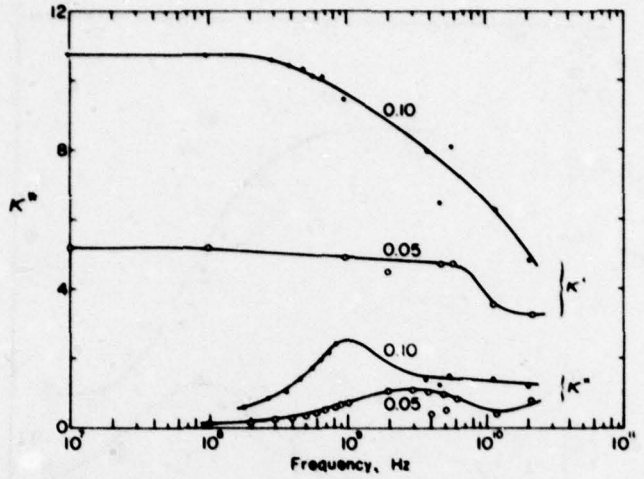

Figure 17. The complex dielectric constant of Goodrich clay at 20°C as a function of frequency at two water contents (g H_2O/g soil).

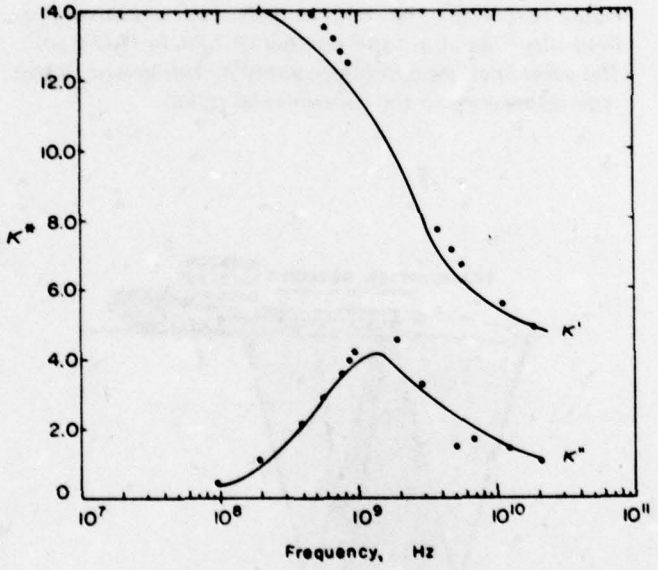

a. 24°C.

Figure 18. The complex dielectric constant of Suffield silty clay at a water content of 10% (g H_2O/g soil). The solid lines are curves generated by fitting two Debye type dispersions to the experimental points.

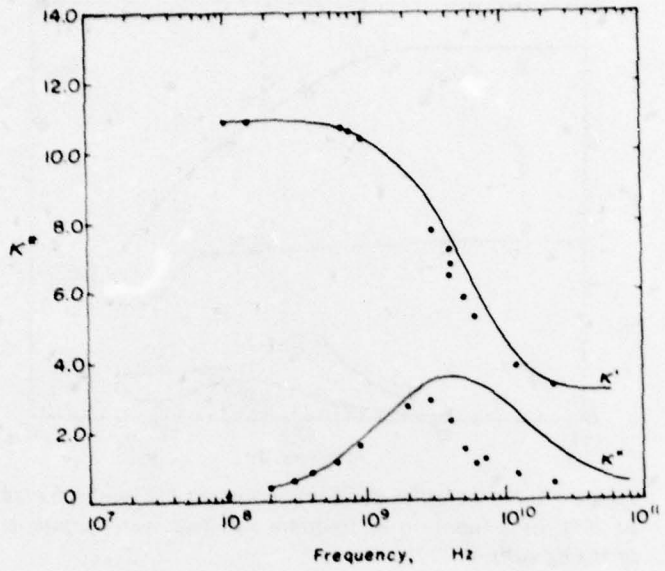

b. −10°C.

Figure 18 (cont'd). The complex dielectric constant of Suffield silty clay at a water content of 10% (g H_2O/g soil). The solid lines are curves generated by fitting two Debye type dispersions to the experimental points.

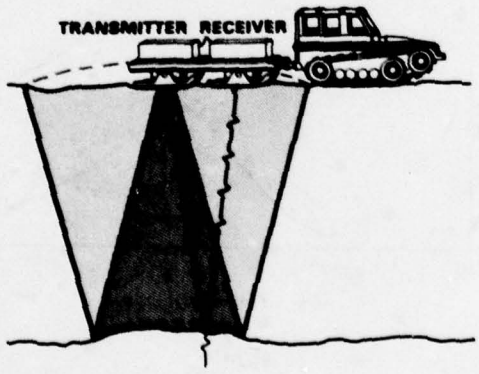

Figure 19. Ground-based impulse radar. The dark shaded area is the transmitted beam and the lighter shading is the reflected beam. The line of impulse waveforms represents the portion of the beam that is received. Time of return is translated into distance.

to 4 for dry silt). Note that at -10°C in Figures 16 and 18b there is appreciable dispersion which is due to the unfrozen adsorbed water. These curves suggest that serious attenuation will take place for radar signals propagating through frozen sediments between 0.1 and 10 GHz.

Dry materials are generally nondispersive, but considerable information is lacking on their behavior at microwave frequencies. Often, the constituent minerals show some degree of anisotropy. At frequencies between 100 Hz and 10 MHz, Parkhomenko (1967) reports that values of κ' most generally fall between 5 and 10 for dry sedimentary rocks with the exception of some shales which are rocks high in clay mineral content. The addition of water to the more porous sedimentary rocks may then cause κ' to increase to as high as 40 (Parkhomenko 1967).

Theory and description of equipment

Profiling radar

Profiling radars have been described in the articles by Moffitt and Puskar (1976), Davis et al. (1976) and Annan and Davis (1976). The principal features and operation of a subsurface profiling radar system are shown in Figure 19. A transmitting and receiving antenna can be mounted on a sled and continuously towed over the ground or ice surface, or it can be attached to a slow flying aircraft. The transmitter radiates a continuous train of pulses that are monitored by the receiver after reflecting from subsurface interfaces. The time and amplitude of return are graphically displayed to produce an apparent profile of the subsurface interfaces. If the dielectric permittivity of the media above the interface is known, delay time can be converted into distance.

In practice, the impulse radiated is about one full sinusoid lasting about 10 to 20 ns. The frequency spectrum is centered at about 100 MHz, which, as was shown in Figures 16-18, is about optimum for minimal ground attenuation. The bandwidth is about 150 MHz. Recently, sinusoidal pulses centered at about 625 MHz have been used over sea ice (Kovacs and Morey 1978). These pulses have bandwidths of about 500 MHz, which allow serious pulse distortion when propagation is in a dispersive material. Therefore, this frequency is best applied in areas containing ice or material that is frozen or of low moisture content.

Ideally, the ground surface as well as the subsurface interfaces should be smooth to avoid noise caused by mechanical vibrations and unwanted signal backscatter (termed clutter). Consequently, best results are often obtained over smooth ice covers.

Imaging radar

Surveillance radars are those that are able to construct two-dimensional images from the time delay and amplitude of the signal return. In geological reconnaissance, a type of surveillance radar used is known as SLAR or side-looking airborne radar, illustrated in Figure 20. In a SLAR system, an antenna fixed beneath an aircraft radiates a beam which is narrow in the direction of the line of flight and broad in the transverse direction. The time of return is simply related to the ground distance and the amplitude is mainly determined by the orientation of the local ground profile with respect to the beam. The width of illuminated terrain is reasonably fixed by the beam shape, and the scanning swaths are parallel with the flight line.

These systems normally operate in the microwave band between 1 and 10 GHz. The radiated signals are a series of pulses containing several hundred or thousand cycles of the microwave frequency. Consequently, beamwidth and bandwidth are well-defined. Since earth materials, even when frozen, can exhibit appreciable loss at these frequencies, most subsurface penetration will occur only through relatively lossless dielectrics like freshwater ice, dry sediment, or snow.

Case studies

Radar profile of a river channel

The Geological Survey of Canada (Annan and Davis 1977) has used the impulse radar technique to profile ice depth and bathymetry beneath an ice road (or bridge) across the Yukon River at Dawson City, Y.T., Canada. Two different profiles were made, one with an impulse of 2-ns duration and one with a 10-ns duration. Figure 21 shows the 2-ns and 10-ns profiles and a geological interpretation. The closely spaced dark bands correspond to the successive maxima of a single impulse return. The thin white lines are the points of zero amplitude within the sinusoidal pulse. The various interfaces with which the returns correspond are labeled in the figure.

In comparing the 2-ns to the 10-ns profile, it is apparent that the 2-ns system does not have the

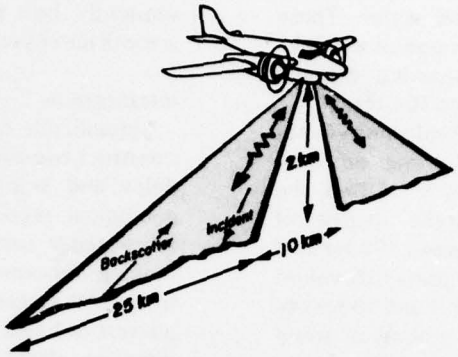

Figure 20. Side-looking airborne radar. Time of return is translated into distance and amplitude of return into image contrasts. Major radiation lobes are shaded. Return energy is backscattered rather than specularly reflected.

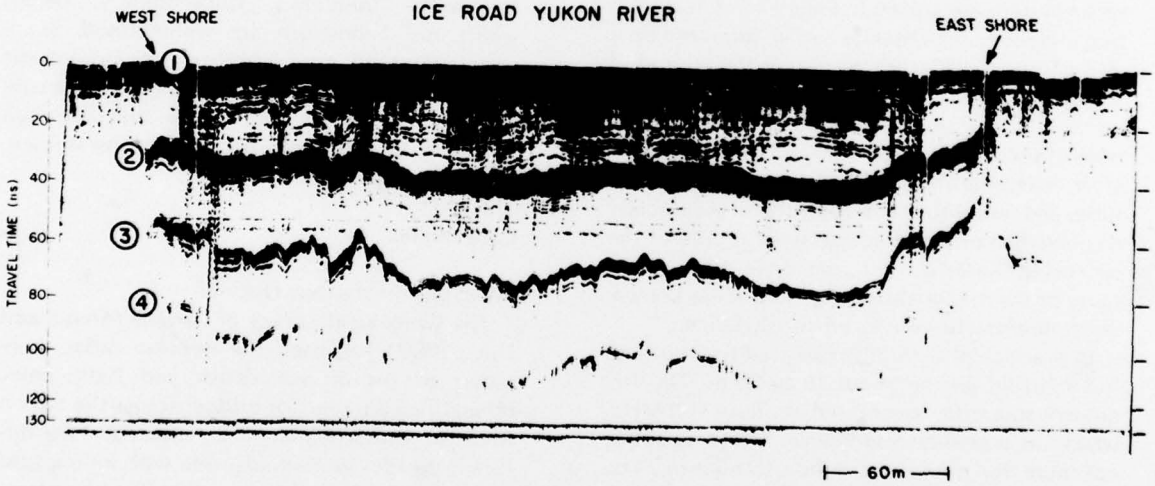

a. Radar section of the ice bridge across the Yukon River obtained with the 2-ns impulse antennas.

Figure 21. Impulse radar profile at 2-ns and 10-ns pulse duration across the Yukon River at Dawson City, Y.T. (courtesy of the Geological Survey of Canada).

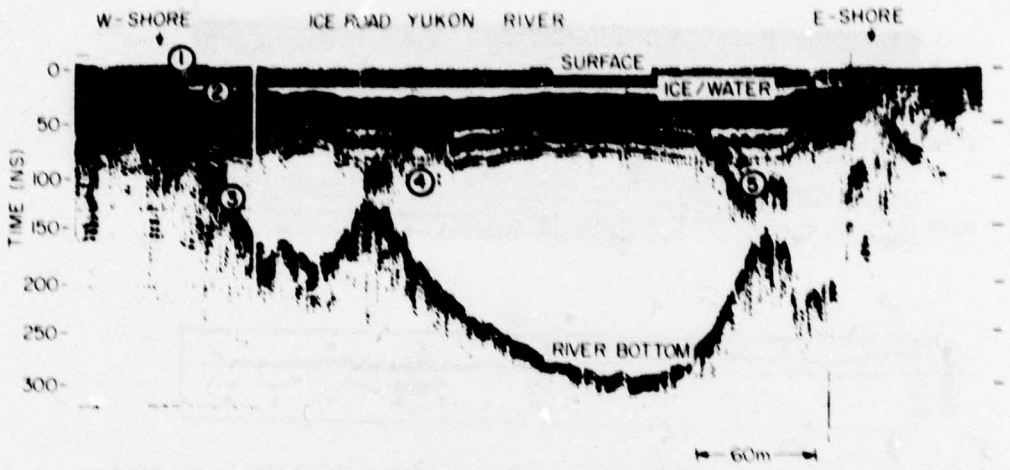

b. Radar section of the ice bridge across the Yukon River obtained with the 10-ns impulse antennas.

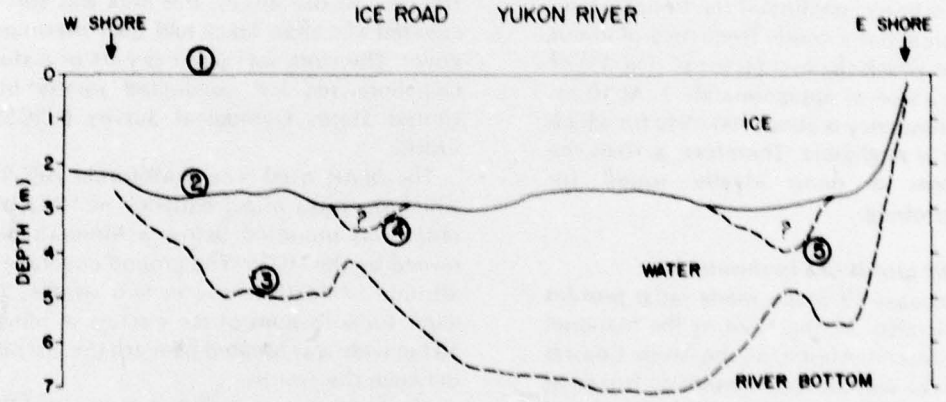

c. Interpretation of the radar sections in Figures a and b.

Figure 21 (cont'd).

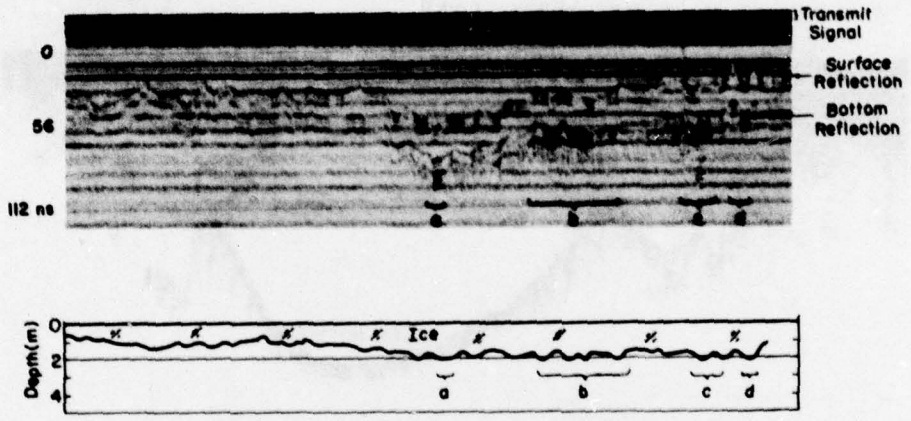

Figure 22. Radar profile obtained from a helicopter over Big Lake on the Alaskan North Slope (after Kovacs 1978). The "bright spots," dark areas on the record, indicate potential sites where water still exists under the ice.

water penetration capability of the 10-ns system. The 2-ns system has a center frequency of about 500 MHz for which the loss factor κ'' (Fig. 15) of water has a value of approximately 1. At 10 ns, the center frequency is about 100 MHz for which κ'' of water is negligible. Therefore, a 10-ns impulse system is more ideally suited for freshwater probing.

Impulse radar profile of a freshwater lake

CRREL (Kovacs 1978) has made radar profiles from a helicopter of Big Lake in the National Petroleum Reserve-Alaska, on the Arctic Coastal Plain. The lake was almost completely frozen at the time of the survey. The radar profile of Figure 22 shows two small areas of strong returns at a two-way time return of 24 ns. This time return corresponds to a depth of 2 m, considering a value of 3.2 for κ' in the ice, which is close to the actual lake depth. A drill hole at the return marked "b" on the figure verified the presence of 4 cm of water between the ice and the lake bed.

SLAR imagery of arctic lakes

During the spring of 1974, SLAR imagery was obtained for part of the Arctic Coastal Plain eastward along the coast from Pt. Barrow, Alaska (Weeks et al. 1977). This area is generally flat and covered with numerous shallow lakes of depths ranging from a few to tens of meters. At the time of the survey, this area was still snow-covered and thaw lakes had their maximum ice cover. The work was done as part of a study of nearshore sea ice conducted jointly by the United States Geological Survey (USGS) and CRREL.

The SLAR used was a Motorola APS-94-XE1 which operates at a frequency of 10 GHz. The radar was mounted below a Mohawk aircraft owned by the USGS. The ground coverage at an altitude of 1830 m was in two swaths, 25 km wide, on both sides of the aircraft. A blind spot 10 km wide was located beneath the aircraft and between the swaths.

The SLAR image of part of the Coastal Plain is shown in Figure 23. An examination of the lake regions reveals that some lakes give strong returns (bright images) while others give weak returns (dark images). Some of the lakes produce strong returns in the central areas but give weak returns around their margins. An interpretation of this difference in returns (see Weeks et al. 1977), which has been verified by limited ground reconnaissance, is as follows. The strong returns are produced at the strong dielectric permittivity contrast between ice ($\kappa = 3.2$) and water ($\kappa' = 60$ at 100 MHz) which exists in the deeper lakes that have not completely frozen. The weak returns indicate areas where no significant subsurface dielectric contrast exists, such as between ice and frozen soil ($4 \leq \kappa' \leq 3$). The

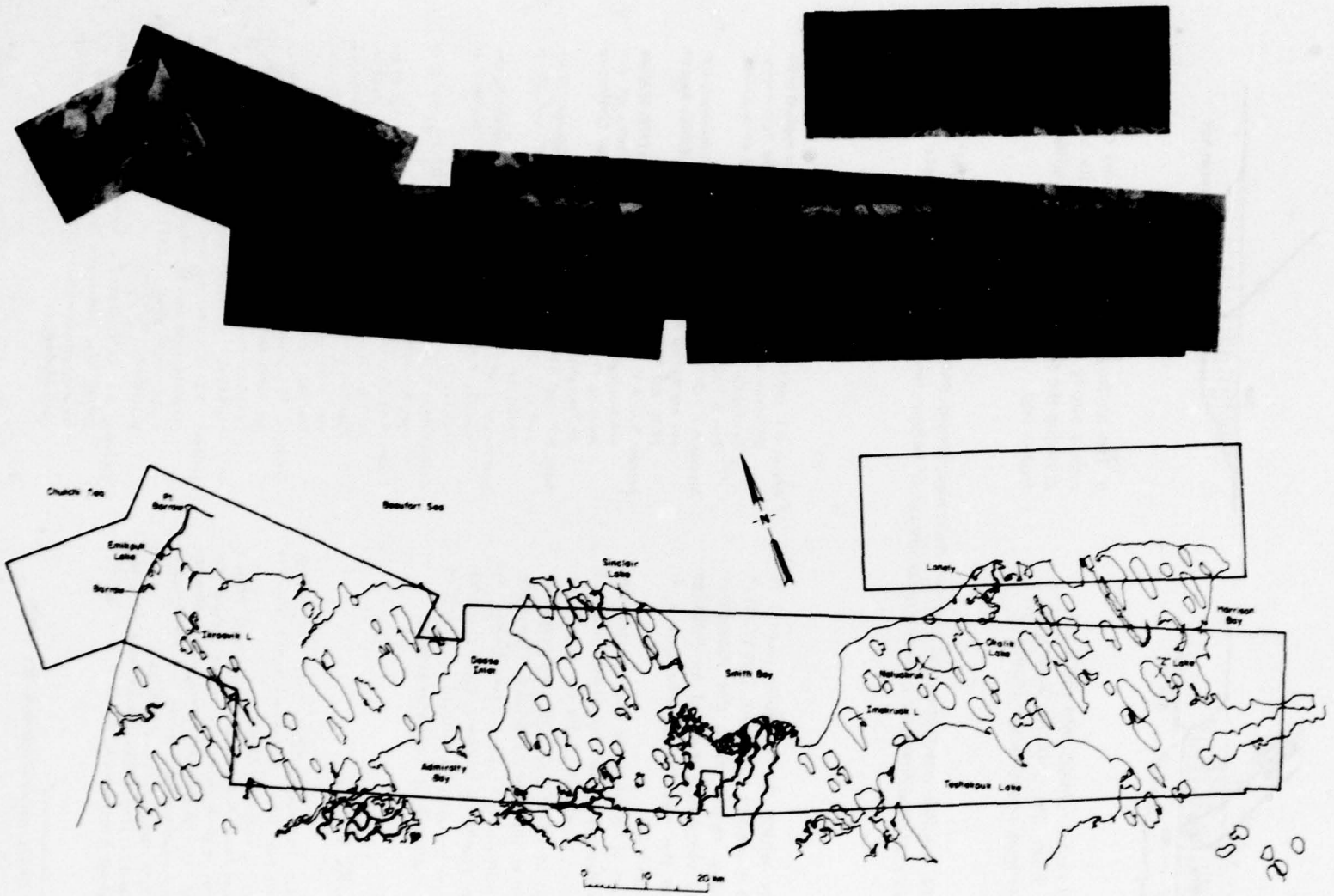

Figure 23. SLAR mosaic of the area between Barrow and Harrison Bay[illegible] a number of the lakes and geographic features identified.

[illegible] map of the area with

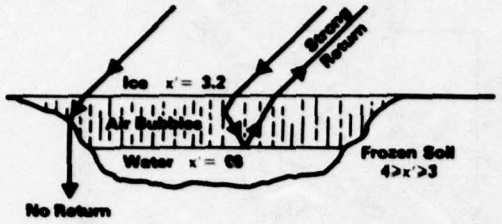

a. The incident signal refracts into the ice, is backscattered from air bubbles and then strongly reflects from the ice/water interface.

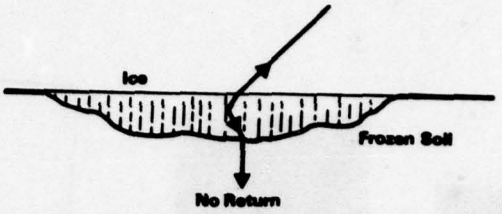

b. The ice/frozen soil interface does not provide a strong dielectric permittivity contrast, allowing the signal to refract strongly into the frozen soil.

Figure 24. Possible wave reflection and refraction mechanisms according to Weeks (1978) that may explain differences between radar images of various lakes on the Arctic Coastal Plain.*

mechanism by which the outgoing signal is backscattered is subject to debate, but Weeks* believes it may result from the numerous elongated and vertically oriented air bubbles trapped within the ice. This mechanism is illustrated in Figure 24.

Although the SLAR imagery appears to contain much information on the distribution of lakes with water available under the ice cover, there is no way in which to determine the quantity of unfrozen water beneath a lake. Therefore, once the appropriate lakes have been determined from the SLAR imagery, ground reconnaissance must be used to determine which of these lakes is best suited for water supply.

LITERATURE CITED

Alaska Highway Department (1973, 1974) Soil borings, Fairbanks-Fox Road centerline. Alaska Highway Department, Fairbanks, Alaska.

Anderson, D.M. and N.R. Morgenstern (1973) Physics, chemistry and mechanics of frozen ground. *Permafrost: Proceedings of an International Conference*, National Academy of Sciences, National Research Council, Washington, D.C., p. 257-288.

Annan, A.P. and J.L. Davis (1976) Impulse radar sounding in permafrost. *Radio Science*, vol. 11, no. 4, p. 383-394.

Annan, A.P. and J.L. Davis (1977) Impulse radar applied to ice thickness measurement and freshwater bathymetry. Geological Survey of Canada, Report of Activities, Part B, Paper 77-1B.

Arcone, S.A. (1977) Investigation of an airborne resistivity survey conducted at very low frequency. CRREL Report 77-20. AD A044684.

Arcone, S.A., P.V. Sellmann and A.J. Delaney (1978) Shallow electromagnetic geophysical investigations of permafrost. *Proceedings, Third International Conference on Permafrost*, Edmonton, Alberta.

Auty, R.P. and R.H. Cole (1952) Dielectric properties of ice and D_2O. *Journal of Chemical Physics*, vol. 20, p. 1309-1314.

Barnes, D.F. (1965) Geophysical methods for delineating permafrost. *Proceedings, First Permafrost Conference*, p. 349-355.

Collie, C.H., J.B. Hasted and D.C. Ritson (1948) *Proceedings of the Philosophical Society*, vol. 60, p. 145.

Culley, R.W., F.L. Jagodits and R.E. Middleton (1975) E-Phase system for detection of buried granular deposits. Paper presented at the Symposium on Modern Innovations in Subsurface Exploration, University of Toronto, Toronto, Canada.

Davis, J.L., W.J. Scott and A.P. Annan (1976) Impulse radar experiments on permafrost near Tuktoyaktuk, N.W.T. *Canadian Journal of Earth Sciences*, vol. 13, p. 1584-1590.

Delaney, A.J., S.A. Arcone and P.V. Sellmann (1977) A magnetic induction technique for shallow subsurface arctic exploration. CRREL Technical Note (unpublished).

Delaney, A.J., D. Gaskin, P.V. Sellmann and P. Hoekstra (1974) New radiowave resistivity techniques for locating groundwater supplies. CRREL Technical Note (unpublished).

*W.F. Weeks, CRREL, personal communication, 1978.

Delaney, A.J., P.V. Sellmann, and P.V. Hoekstra (1975) Alaska pipeline ground resistivity study. Part 2: Yukon River to Prudhoe Bay. CRREL Internal Report 471.

Hoekstra, P. and J.D. McNeill (1973) Electromagnetic probing of permafrost in the North. *Permafrost: Proceedings of an International* Conference, National Research Council, National Academy of Sciences, p. 517.

Hoekstra, P., P.V. Sellmann and A.J. Delaney (1974) Airborne resistivity mapping of permafrost near Fairbanks, Alaska. CRREL Research Report 324, AD A000694.

Hoekstra, P., and A. Delaney (1974) Dielectric properties of soils at UHF and microwave frequencies. *Journal of Geophysical Research*, vol. 75, no. 11.

Hopkins, D.M., T.N.V. Karlstrom et al. (1955) Permafrost and groundwater in Alaska. Geological Survey Professional Paper 264-F, U.S. Geological Survey.

Jackson, J.D. (1962) *Classical electrodynamics*. New York: John Wiley.

Keller, G.V. and F.C. Frischknecht (1966) *Electrical methods in geophysical prospecting*. New York: Pergamon Press.

Kovacs, A. (1978) Detection of water under ice-covered lake on the North Slope of Alaska. *Arctic*, December 1978.

Kovacs, A. and R.M. Morey (1978) Radar anisotropy of sea ice due to preferred azimuthal orientation of the horizontal c-axes of ice crystals. *Journal of Geophysical Research*, vol. 83, C12.

Moffitt, D.L. and R.J. Puskar (1976) A subsurface electromagnetic pulse radar. *Geophysics*, vol. 41, no. 3, p. 506-518.

Northern Engineering Services Company Limited (1976, 1977) Geophysical survey of rivers of the Arctic Coastal Plain in the Yukon Territory. Northern Engineering Services, Calgary, Alberta, Canada. Appendix A.

Ogilvy, A.A. (1967) Geophysical prospecting for groundwater in the Soviet Union. Geological Survey of Canada, Economic Geology Report. 26, p. 641-650.

Parkhomenko, E.I. (1967) *Electrical properties of rocks* (translated from Russian by G.V. Keller). New York: Plenum Press.

Péwé, T.L. (1958) Geology of the Fairbanks (D-2) Quadrangle, Alaska. U.S. Geological Survey Geological Quadrangle Map GQ-110.

Polcyn, F.C. and Lyzenga (1973) Updating coastal and navigational charts using ERTS-1 data. In *Proceedings from Third Earth Resources Technology Satellite Symposium*, p. 1333-1346.

R & M Engineering and Geological Consultants (1970) Special soil profile study, Copper River Basin, Alaska, Fairbanks, Alaska.

Scott, W.J. and J.A. Hunter (1976) Applications of geophysical techniques in permafrost regions. *Canadian Journal of Earth Sciences*, vol. 14.

Sellmann, P.V., P. Hoekstra and A. Delaney (1974) Electrical resistivity measurements at Alaska Pipeline Pump Stations 1 through 5. CRREL Internal Report 409.

Sellmann, P.V., J. Brown, R.I. Lewellen, H. McKim and C. Merry (1975) The classification and geomorphic implications of thaw lakes on the Arctic Coastal Plain, Alaska. CRREL Research Report 344, ADA021226.

Stratton, J.A. (1941) *Electromagnetic theory*. New York: McGraw-Hill.

Ward, S.H. (Ed.) (1967) Electrical methods. In *Mining Geophysics*, vol. II, pt. B, p. 198-223, Society of Exploration Geophysicists, Tulsa, Oklahoma.

Wait, J.R. (1962) *Electromagnetic waves in stratified media*. New York: Pergamon Press.

Weeks, W.F., P.V. Sellmann and W.J. Campbell (1977) Interesting features of radar imagery of ice covered North Slope lakes. *Journal of Glaciology*, vol. 18, no. 78.

Zohdy, A.A.R., G.P. Eaton and D.R. Mabey (1974) Application of surface geophysics to groundwater investigation. In *Techniques of Water Resources Investigation*, U.S. Geological Survey, p. 116.

APPENDIX A. SATELLITE IMAGERY FOR SUBSURFACE WATER EXPLORATION

In this section we discuss the use of satellite imagery at optical wavelengths for subsurface arctic water exploration. Subsurface water is inferred from surface features which indicate whether or not a lake is totally frozen. Although optical imaging is technically an electromagnetic technique, it is discussed in an appendix because, in contrast to most other geophysical techniques, it is passive and has marginal earth penetration. It is also subject to weather conditions.

This discussion is taken from a larger study by Sellmann et al. (1975) of ERTS-1 (Earth Resources Technology Satellite) imagery. The images were obtained throughout the spring thaw of 1973 at MSS (multi-spectral scan) band 5 (0.6-0.7 μm wavelength) and band 7 (0.8-1.1 μm) and are of the same Arctic Coastal Plain Region shown in Figure 23. The features of interest in this figure are the lakes that are deep enough to retain subsurface water during the winter. The lakes were divided into three general depth categories based on changes seen in sequential imagery obtained throughout the thaw period and on differences detected between bands 5 and 7. The categories are 1) lakes in excess of 2-m depth that do not freeze to the bottom, 2) shallow lakes of intermediate depth (1-2 m) that freeze to the bottom, and 3) very shallow lakes and ponds (<1 m), some of which are basins that are seasonally filled at the time of spring runoff.

The first depth class (>2 m) contains the important lakes in terms of providing winter water supplies. This depth class can be detected by observing whether or not a lake in question has retained its ice cover long after the shallow lakes have become ice-free. During June and early July, an open water moat corresponding to the shallow water areas usually forms around the remaining ice of the deeper central basin which can be as much as 2 m thick. Figures A1 (June) and A2 (July) at band 7 show that the decrease in size of the persisent ice masses can be followed if cloud cover permits adequate sequential coverage.

The second depth class (1-2 m), less obvious than the first group, includes shallow lakes that have frozen to the bottom, usually throughout their basins. In Figure A3 at band 7, these lakes appear dark, suggesting no ice cover such as noted in the vicinity of Sinclair Lake. However, this class of lakes appears white at band 5. The difference appears to be caused by the greater penetration of band 5 wavelengths through the ice flooding caused by surface runoff [penetration of light through water for band 5 radiation has been reported to be as great as 3 m (Polcyn and Lyzenga 1973)]. If the lakes were not frozen to the bottom, the ice mass would float and not be subjected to surface runoff, thereby eliminating the contrast betwen bands 5 and 7.

The third depth class (<1 m) consists of shallow lakes that appear dark on bands 5 and 7 early in the melt season. The shallow depths of these lakes allow the ice to completely melt quite early and therefore produce no contrasts between the different wavelength images.

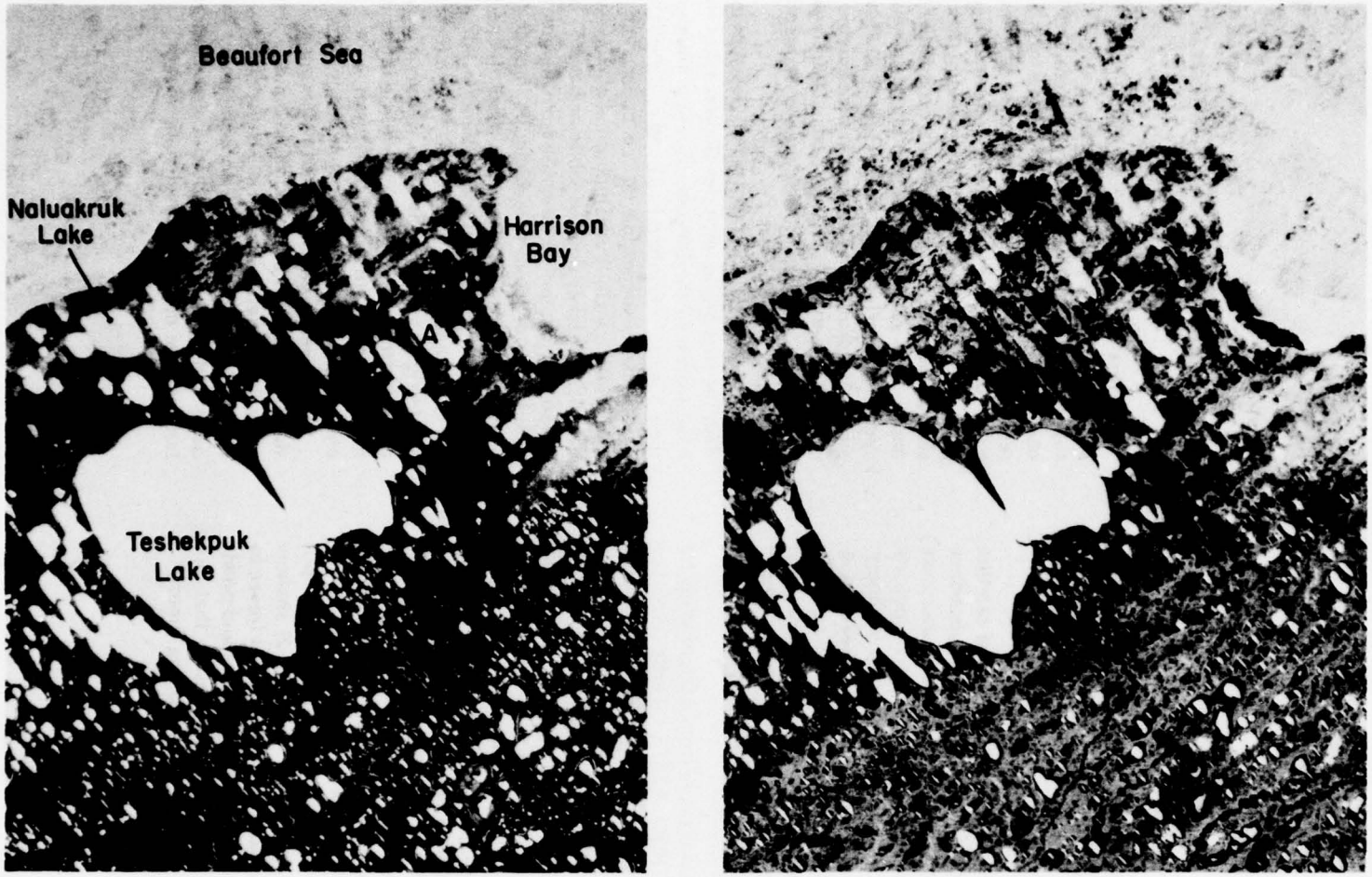

Figure A1. ERTS-1 imagery of the Teshekpuk Lake region obtained on 17 June 1973 (NASA ID no. E-1329-2145), with band 5 (0.6-0.7 μm) on the left and band 7 on the right. Comparison of Figure A1 and A2 indicates dissipation of lake ice cover with time.

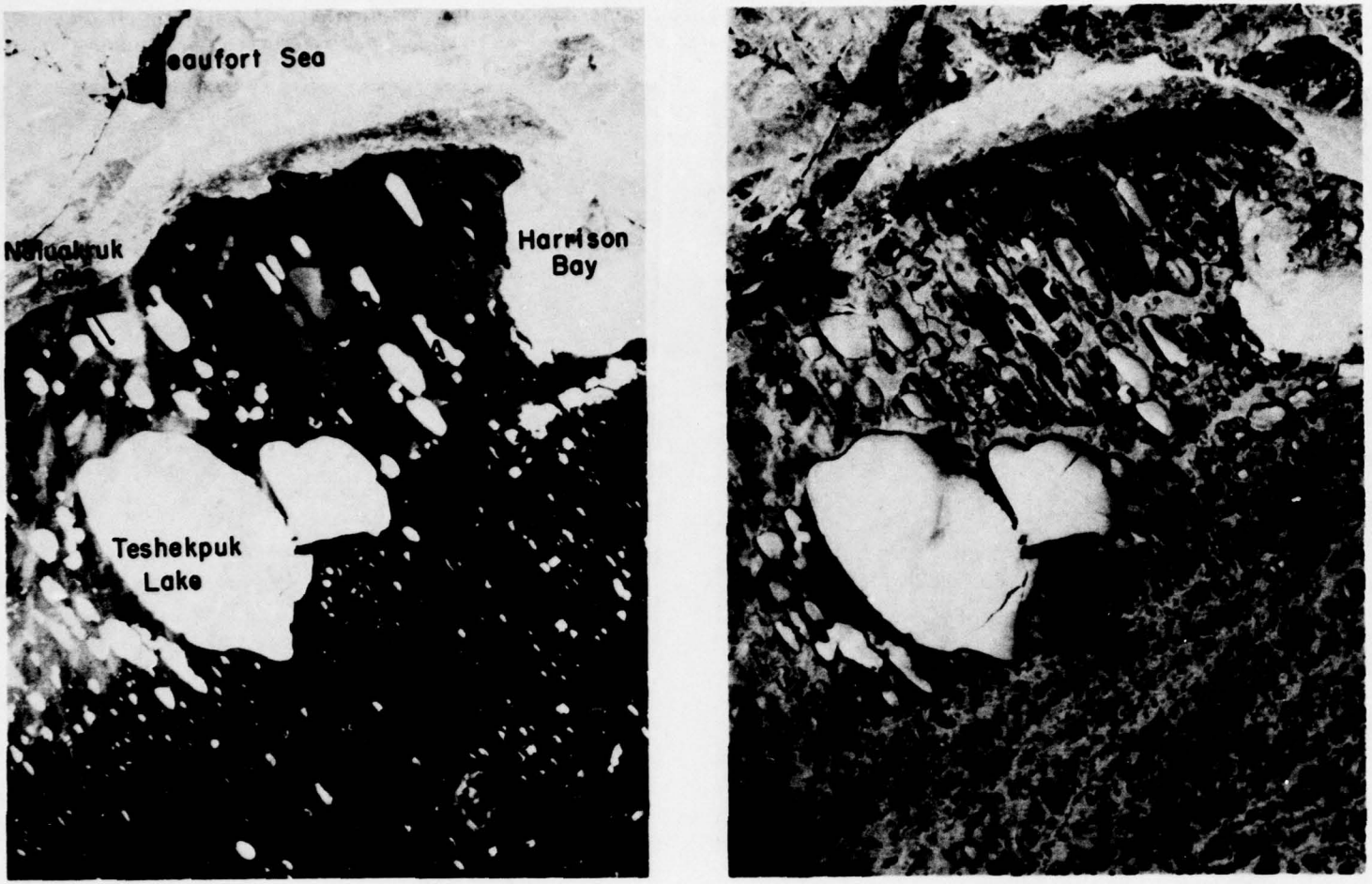

Figure A2. ERTS-1 imagery of the same area shown in Figure A1 obtained on 3 July 1973 (NASA ID no. E-1345-21342), with band 5 on the left and band 7 on the right.

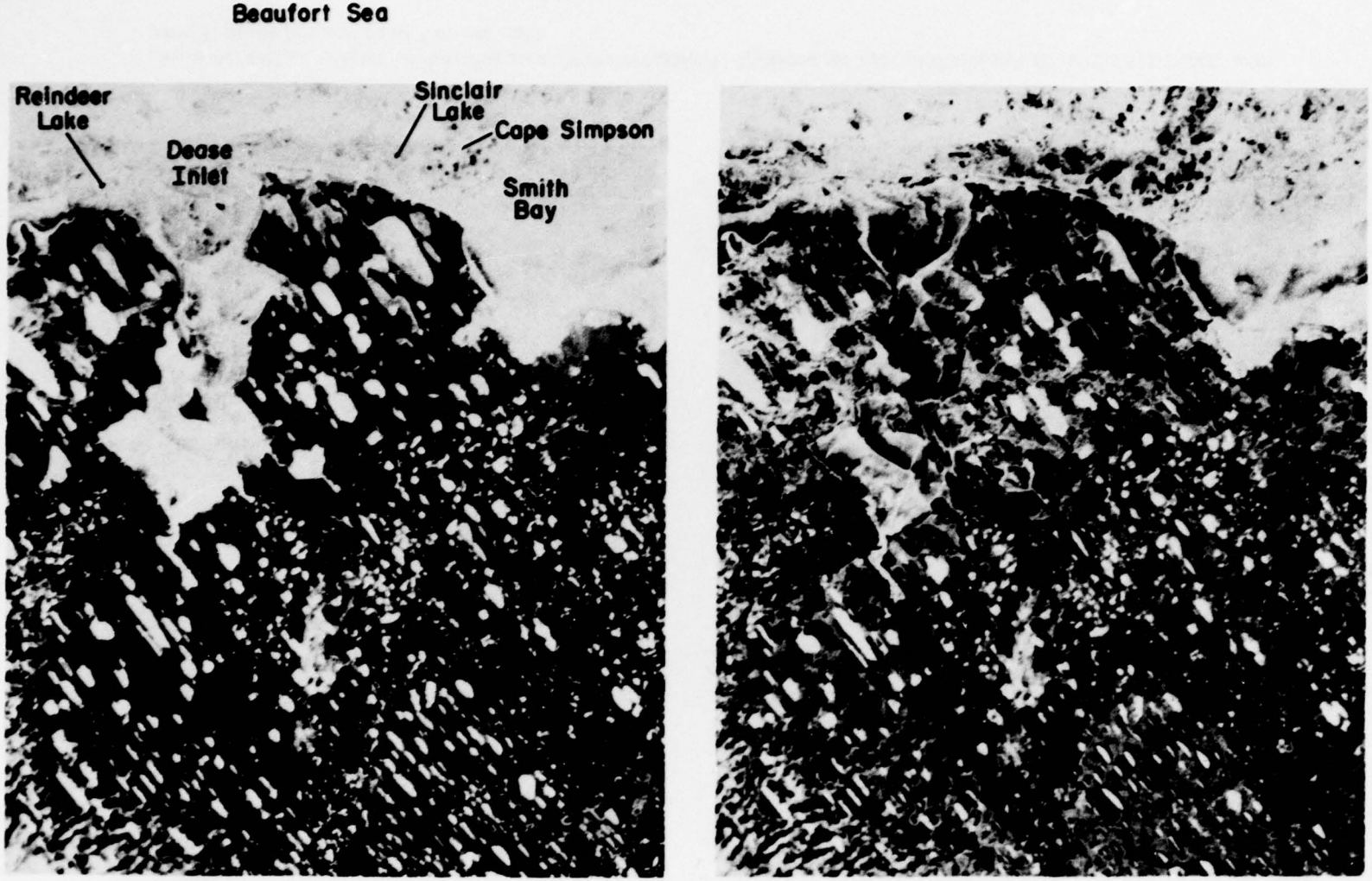

Figure A3. ERTS-1 imagery of a section of the Arctic Coastal Plain near Cape Simpson obtained on 17 June 1973 (NASA ID no. E-1329-21455). Band 5 imagery is shown on the left and band 7 shown on the right for comparative purposes. Note the contrast in tone between the lakes to the southeast of Sinclair Lake.

A facsimile catalog card in Library of Congress MARC format is reproduced below.

Arcone, S.A.
Detection of arctic water supplies with geophysical techniques / by S.A. Arcone, A.J. Delaney and P.V. Sellmann. Hanover, N.H.: U.S. Cold Regions Research and Engineering Laboratory; Springfield, Va.: available from National Technical Information Service, 1979.
iv, 34 p., illus.; 27 cm. (CRREL Report 79-15.)
Prepared for Directorate of Military Programs, Office, Chief of Engineers by Corps of Engineers, U.S. Army Cold Regions Research and Engineering Laboratory under DA Project 4A762730AT42.
Bibliography: p. 24.
1. Arctic regions. 2. Electrical resistivity. 3. Geophysics. 4. Water supplies. I. Delaney, A.J. II. Sellmann, P.V. III. United States. Army. Corps of Engineers. IV. Army Cold Regions Research and Engineering Laboratory. V. CRREL Report 79-15.

☆ US GOVERNMENT PRINTING OFFICE: 1979—601-534/96